

# Guidelines when estimating temporal changes in density dependent populations



Erik Blystad Solbu<sup>a,\*</sup>, Steinar Engen<sup>a</sup>, Ola Håvard Diserud<sup>b</sup>

<sup>a</sup> Centre for Biodiversity Dynamics, Department of Mathematical Sciences, Norwegian University of Science and Technology, N-7491 Trondheim, Norway

<sup>b</sup> Norwegian Institute for Nature Research, N-7485 Trondheim, Norway

## ARTICLE INFO

### Article history:

Received 14 April 2015

Received in revised form 17 June 2015

Accepted 24 June 2015

Available online 30 July 2015

### Keywords:

Theta-logistic model

Ornstein–Uhlenbeck process

Time dependent parameters

Sample size

Range

Bayesian analysis

## ABSTRACT

Anthropogenic activity can cause changes in the population dynamics of species. The changes can be modelled by density dependent models with time varying parameters. The following study looks at the accuracy of model parameter estimates using primarily simulations, in addition to a real data set of Grey Heron. A key point is the amount of data required to detect deterministic changes, either step-wise or gradual, in parameters for species with different population dynamics. The theta-logistic model is used to simulate the data and fitted to realizations of step-wise change in growth rate, and a linear model is fitted to gradual or step-wise changes in carrying capacity. Bayesian analysis is applied to study the effect of different prior distributions on the strength of density regulation. The range of the data is especially important when trying to detect step-wise changes in growth rate. Detection of changes in carrying capacity depends on the dynamics of the population, e.g. it is difficult to observe change for species with long return time to equilibrium within short time frames. The estimates of change in carrying capacity can become more accurate using a strong prior on the strength of density regulation. However, the prior may give more conservative estimates, if the prior assumes a weak density regulation. The results provide ecologists and decision makers with a general idea of what to expect of analyses of time series data of populations in changing environments.

© 2015 Elsevier B.V. All rights reserved.

## 1. Introduction

In population ecology, stochastic density dependent models are used to describe fluctuations in population size and ultimately predict how species are expected to persist in the future. Some species have a large growth rate and are able to increase their abundance rapidly after environmental perturbations, while other species produce fewer offspring, are less abundant and will have a slow return to carrying capacity. The range of possible species dynamics can be described by different parameterizations of the stochastic population models. Provided that the model used is reasonable, the inference about the species dynamics is based on some method of estimation. The estimation methods often assume that the environment of the species is stationary, which means that the parameters of the stochastic models are constant over the time period the species is observed. The stationary assumption may be reasonable over shorter time intervals, or when there is no reason to believe that any changes to the environment have occurred.

However, anthropogenic activity can create a non-stationary environment, causing temporal changes in population parameters, such as habitat reduction because of deforestation, change in number of offspring due to food availability, change in age of maturity following harvesting and greater variation in weather conditions as a consequence of climate change. When the cause of the potential change in population dynamics is assumed to be known, deterministic changes in the parameters can be considered, e.g. step-wise change at a known time point. How temporal changes in different model parameters can affect the dynamics of a density dependent population have been discussed in Solbu et al. (2013). Basically, the species' response to change in the parameters depends on the initial dynamics of the species, so that those with high reproduction/short lifetime respond quicker to change than those with low reproduction/long lifetime. Because species specific characteristics determine the response to change in the environment, it is important to assess how accurately these parameters, in addition to any temporal change, can be estimated.

Several methods are available for estimating parameters in density dependent population models, both when the relationship between growth rate and log population size is linear (Dennis et al., 2006; Dennis and Ponciano, 2014) and non-linear (Wang, 2007;

\* Corresponding author. Tel.: +47 97584012.  
E-mail address: [erik.solbu@math.ntnu.no](mailto:erik.solbu@math.ntnu.no) (E.B. Solbu).

Pedersen et al., 2011). These approaches account for observation error and include both frequentist and Bayesian methods. Following Bolker et al. (2013), the software and packages applied in this work are straightforward to use for ecologists and can be easily checked and modified. The non-linear model uses a slightly modified JAGS procedure as described by Pedersen et al. (2011) and Bolker et al. (2013), while the linear model uses the Integrated Nested Laplace Approximation (INLA) (Rue et al., 2009). Both methods are within the Bayesian framework so that the effect prior knowledge have on the estimated temporal changes can be investigated. The difficulties with non-stationary time series, and the pitfalls of the common de-trending approach, is well known in ecology (Turchin, 2003). While a time series can indicate a trend in abundance, the observations could simply be caused by a natural perturbation of a species with long return time to equilibrium. Similarly, failing to account for a trend could result in over-estimating the return time to equilibrium of the species. A remedy for separating a trend in abundance from natural long perturbations away from equilibrium is obtaining a larger sample size. However, acquiring more observations is often impossible in ecology, e.g. when assessments of species viability must be made now, as a basis for management of natural resources. The goal of this work is to quantify the challenges of detecting change in a population parameter using simulations. Realistic sample sizes of biological data, and different population dynamics of species, are key aspects that will be investigated. In addition, the effect of sampling error and prior knowledge on the species' parameters will be studied. Finally, the range of the data will be considered, i.e. whether the population abundance is observed in a growth phase from small population size up to carrying capacity, or only observed fluctuating around the equilibrium.

## 2. Materials and methods

### 2.1. Theta-logistic model with time varying parameters

The theta-logistic population model (Gilpin and Ayala, 1973), can be approximated by a diffusion process, provided that the yearly fluctuations are small or moderate (20–30%) (Lande et al., 2003),

$$dN_t = \mu_N(n)dt + \sqrt{v_N(n)}dB_t \quad (1)$$

where the infinitesimal mean is  $\mu_N(n) = r_1 n [1 - (n^\theta - 1)/(K^\theta - 1)]$  for  $\theta > 0$  and  $\mu_N(n) = r_1 [1 - \ln(n)/\ln K]$  for  $\theta = 0$ , which is the Gompertz model (Gompertz, 1825). Here  $r_1$  is the growth rate at population size  $N = 1$ ,  $\theta$  the shape of density regulation and  $K$  the carrying capacity, defined as the population size where the deterministic growth rate is equal to zero. The fluctuations in population size are caused by environmental and demographic stochasticity, modeled by the infinitesimal variance as  $v_N(n) = \sigma_e^2 n^2 + \sigma_d^2 n$ , where  $\sigma_e^2$  and  $\sigma_d^2$  are the environmental and demographic variance, respectively. The environmental variance is defined as the variation in mean individual fitness across years, while the demographic variance is the mean variation in individual fitness within years (Engen et al., 1998). Equation (1) transformed to the log scale  $X_t = \ln N_t$  becomes

$$dX_t = \mu_X(x)dt + \sqrt{v_X(x)}dB_t \quad (2)$$

where  $\mu_X(x) = r_1 [1 - [(e^x)^\theta - 1]/[K^\theta - 1]] - (\sigma_e^2 + \sigma_d^2/e^x)/2$  for  $\theta > 0$ ,  $\mu_X(x) = r_1 [1 - x/\ln K] - (\sigma_e^2 + \sigma_d^2/e^x)/2$  for  $\theta = 0$  and  $v_X(x) = \sigma_e^2 + \sigma_d^2/e^x$ . The example of deterministic temporal change in the parameters considered for the theta-logistic model, substituting  $\mu_X(x)$  by  $\mu_X(x, t)$  in Eq. (2), is a step-wise change in growth rate, replacing  $r_1$  by  $r_1(t) = r_1 I_{(t \geq s)}$ . Here,  $I$  is an indicator

function equal to one if true and zero otherwise, and  $s$ , which is assumed to be known, is the first time point after the parameter value is altered. The proportional change is determined by  $\rho > 0$ , where  $\rho < 1$  and  $\rho > 1$  are decrease and increase in growth rate, respectively.

### 2.2. Linearized model with time varying parameters

The linearization of  $\mu_X(x)$  around  $\ln K$  is  $\mu_X^*(x) = \beta(\alpha_0 - x)$  where  $\alpha_0 = \ln K - (\sigma_e^2 + \sigma_d^2/K)/[2\gamma + \sigma_d^2/K]$  and  $\beta = \gamma + \sigma_d^2/(2K)$  for  $\theta > 0$  and where  $\gamma = r_1 \theta / (1 - K^{-\theta})$  is the strength of density regulation (May, 1981). For the Gompertz model,  $\alpha_0 = \ln K - (\sigma_e^2 + \sigma_d^2/K)/(2r_1/\ln K + \sigma_d^2/K)$  and  $\beta = r_1/\ln K + \sigma_d^2/(2K)$ , thus  $\mu_X(x) = \mu_X^*(x)$ . When demographic variance is assumed to be zero, the linearized model is known as an Ornstein–Uhlenbeck process (Karlin and Taylor, 1981). Since  $r_1$  is confounded with  $\theta$  by the return time  $\approx r_1 \theta$ , the analysis for this model is limited to step-wise and gradual changes in carrying capacity, where the changes are parametrized by replacing  $K$  with  $K(t) = K \kappa^{l_{(t \geq s)}}$  and  $K(t) = K \kappa^t$ , respectively. The magnitude of change is determined by  $\kappa > 0$ , where  $\kappa < 1$  and  $\kappa > 1$  expresses decrease and increase in carrying capacity, respectively. When demographic variance is accounted for,  $K$  occurs in the denominator of both  $\alpha_0$  and  $\beta$ . To simplify the calculations, the fraction  $\sigma_d^2/K$  is approximated by  $\sigma_d^2/\bar{K}$ , where  $\bar{K}$  is the average carrying capacity:  $\bar{K} = K[s + (n - s)\kappa]/n$  or  $\bar{K} = [K \sum_{t=0}^n \kappa^t]/n$  for step-wise and gradual change, respectively. The resulting time varying infinitesimal mean is,  $\mu_X^*(x, t) = \beta(\alpha_0 + I_{(t \geq s)}\alpha_1 - x)$  for the step-wise and  $\mu_X^*(x, t) = \beta(\alpha_0 + t\alpha_1 - x)$  for gradual change in carrying capacity, where  $\alpha_1 = \ln \kappa$ . A detailed discussion of the dynamics of temporal changes in carrying capacity and other parameters for the linear model is found in Solbu et al. (2013).

### 2.3. Estimation

Although demographic variance is defined in the model, time series of species abundance contains no information about individuals' number of offspring or survival from one census to the next, which is needed to estimate demographic variance with some accuracy (Engen et al., 1998). Therefore, it is assumed that demographic variance can be estimated from individual data from the population or similar populations, or from expert information, and used as a known parameter in the model. Ignoring the effect of demographic variance could result in over-estimation of the environmental variance in the population (Sæther et al., 2000). However, if the population is above  $10\sigma_d^2/\sigma_e^2$ , the effect of demographic variance is usually negligible (Lande et al., 2003).

To account for measurement uncertainty of population size, the observed log abundance  $Y_t$  is assumed normally distributed with expectation  $X_t$  and variance  $\tau^2$ , corresponding to the coefficient of variation being approximately constant (Seber, 1982). There are several methods available, both frequentistic and Bayesian, for estimating the parameters in non-linear state-space, or hierarchical, models such as the theta-logistic model, giving similar results for large sample sizes ( $n = 200$ ) (Wang, 2007; Pedersen et al., 2011). Following the guidelines by Bolker et al. (2013), extensively used estimation methods are chosen, which are simple to examine and modify by other researchers. Since one of the objectives is to study the effect of incorporating prior knowledge from biologists and ecologists, Bayesian inference must be applied. For the theta-logistic model, a modification of the code provided by the National Center for Ecological Analysis and Synthesis web site (Bolker et al., 2013) is applied using JAGS (Plummer, 2003) and run in R (R Core Team, 2014).

The parameters of the linear model are estimated using the Integrated Nested Laplace Approximation (INLA) method (Rue et al.,

**Table 1**

A summary of the different changes in parameter values that is considered the simulated cases. The step-wise change is 50% in the described directions, while the gradual changes are 2% each unit time. The initial parameter values for  $r_1 = 0.2$  and  $K = 1000$ . ‘Low’ initial abundance is  $N = 20$ , while ‘K’ indicates starting at carrying capacity.

Case	A	B	C	D	E	F	G	H	I	J	K
Change					Step-wise						Gradual
Parameter				$r_1$							
Direction				Decrease							
Initial abundance	Low	K	Low <sup>a</sup>				Increase	K	Decrease		
Density dependence		Strong	Weak			Strong	Weak	K	Strong	Weak	Increase
								Strong	Weak	Strong	Weak

<sup>a</sup> Here, the population size is reduced down to ‘Low’ abundance right after the change in  $r_1$  in order to observe the population having a ‘growth phase’ after the change. ‘Strong’ and ‘Weak’ density dependence corresponds to  $\theta = 1.5$  and 0.5, respectively. The other parameter values are  $\sigma_e^2 = 0.01$ ,  $\sigma_d^2 = 0$  and  $\tau^2 = 0.01$ .

2009), which has the Ornstein–Uhlenbeck model readily available (see [www.r-inla.org](http://www.r-inla.org)). The observed log population counts  $Y_{t_0}, Y_{t_1}, \dots, Y_{t_n}$  at (arbitrary) time points are then assumed to be normally distributed  $N(\eta_i, \tau^2)$ . The mean  $\eta_i$  is a link function structured in an additive way  $\eta_i = \alpha + f(t_i)$ , where  $f(t_i)$  are Gaussian with mean  $X_{t_{i-1}} \exp(-\beta \delta_i)$ , where  $\delta_i = t_i - t_{i-1}$  and variance  $[\sigma_e^2/(2\beta)](1 - \exp(-2\beta\delta_i))$ , for  $i = 1, \dots, n$ . The marginal distribution of  $X_{t_0}$  is assumed to be the stationary distribution  $N(\alpha, \sigma_e^2/[2\beta])$ . The step-wise change in carrying capacity is modeled as two separate time series with the same latent diffusion process, but with different intercepts (fixed effects), e.g. if the step-wise change occurs at time  $t_s$ , the mean  $\eta_i = \alpha_0 + f(t_i)$ , for  $t_0, \dots, t_{s-1}$  and  $\eta_i = \alpha_0 + \alpha_1 + f(t_i)$  for  $t_s, \dots, t_n$ . The gradual change is similarly modeled as a single diffusion process with a fixed linear trend,  $\eta_i = \alpha_0 + \alpha_1 t_i + f(t_i)$ . The biological parameters are straightforward to compute from the diffusion parameters and details are found in Appendix A.

The prior distributions for the theta-logistic model follows Pedersen et al. (2011), where the priors on the environmental and

sampling variances are inverse gamma distributed, and with the additional parameter  $\rho$ , the proportional change in growth rate, which is uniformly distributed on the log scale on the interval  $(-4, 2)$ . The linear model uses the default priors of INLA (see [www.r-inla.org](http://www.r-inla.org)). In addition, the effect of a strong prior on  $\beta$  for the linear model is studied. The strong prior on  $\beta$  represents biological knowledge the researcher might have about the species, such as the average number of offspring per year or the age at maturity. In this work, the prior distributions of  $\beta$  are normal on the log scale with expectation  $\log \gamma$  and variances equal to 0.01. For example, a species with strength of density regulation equal to 0.3, the mean return time to equilibrium is 3.3 years and this prior distribution would correspond to a 95% interval between 2.7 and 4 years. Similarly, if  $\gamma = 0.1$ , the interval is between 8.2 and 12.2 years. For the examples using the non-linear model, the mode of the posterior distribution (MAP) is used as point estimate (Pedersen et al., 2011) while the linear models use the mean.

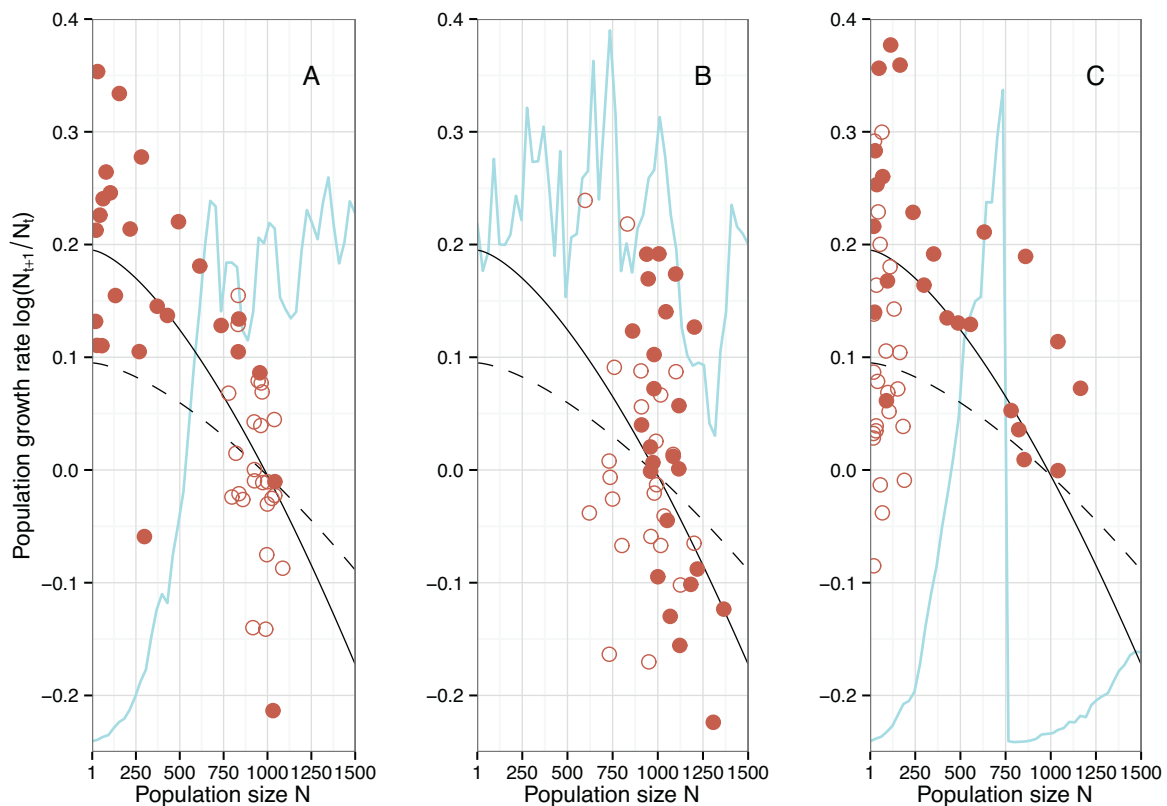


**Fig. 1.** Information contained in time series data of a step-wise change in  $r_1$ . The points are sample population growth rates,  $\Delta X$ , before (●) and after (○) the change. The lines are the stochastic growth rate before (solid) and after (dashed) the change. In the background are schematic illustrations of the population time series with the arithmetic scale (range 0–1400) on the y-axis and time (range 1–50) on the x-axis. The parameter values are  $r_1 = 0.2$ ,  $\rho = 0.5$ ,  $\theta = 1.5$ ,  $K = 1000$  and  $\sigma_e^2 = 0.01$ . The change in growth rate occurs at  $s = 26$  and total sample size is  $n = 50$ . In A and C the initial population size is  $N_0 = 20$ . In B the initial population size is  $N_0 = K$ . In C the population size is reduced to 20 at  $t = s$ , i.e. at the point where the growth rate is halved.

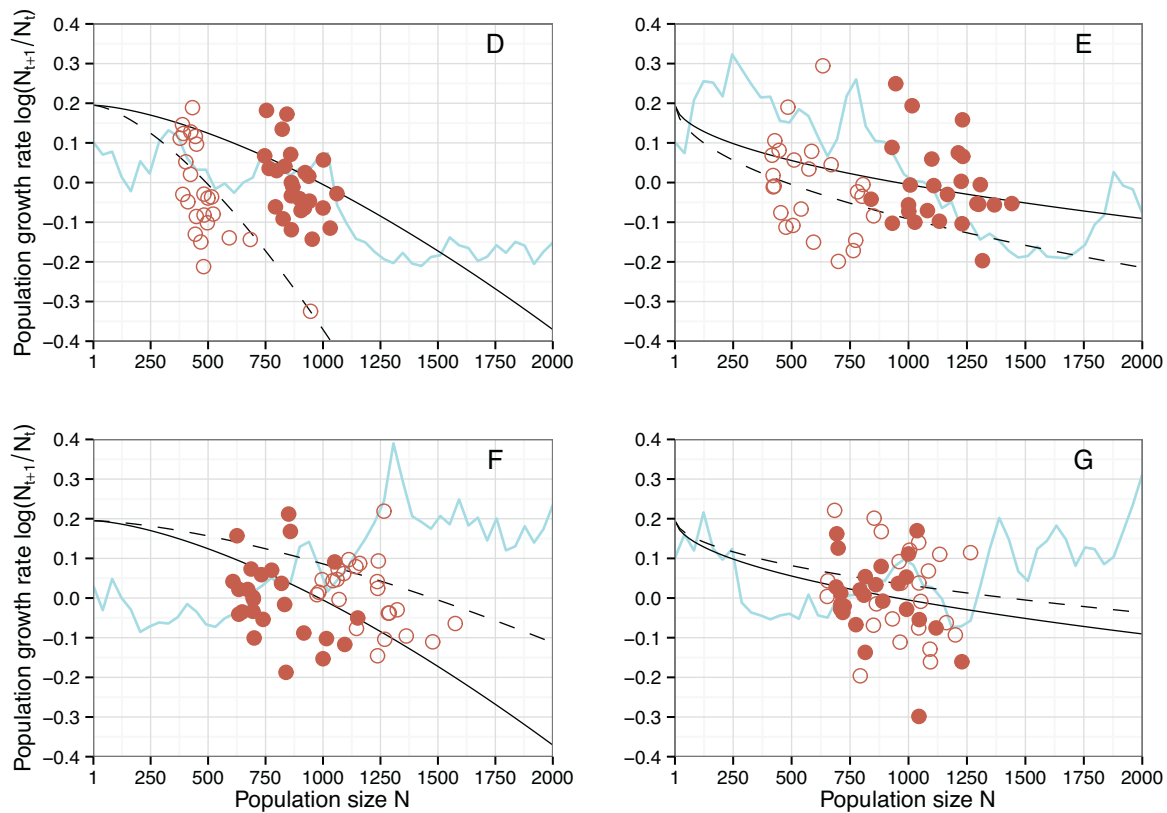


**Fig. 2.** Information contained in time series data of a step-wise change in  $K$ . The points are sample population growth rates,  $\Delta X$ , before (●) and after (○) the change. The lines are the stochastic growth rate before (solid) and after (dashed) the change. In the background are schematic illustrations of the population time series with the arithmetic scale (range 0–1300) on the y-axis and time (range 1–50) on the x-axis. In D and E,  $\kappa = 0.5$ . In F and G,  $\kappa = 1.5$ . In all cases  $r_1 = 0.2$ ,  $K = 1000$  and  $\sigma_e^2 = 0.01$ .

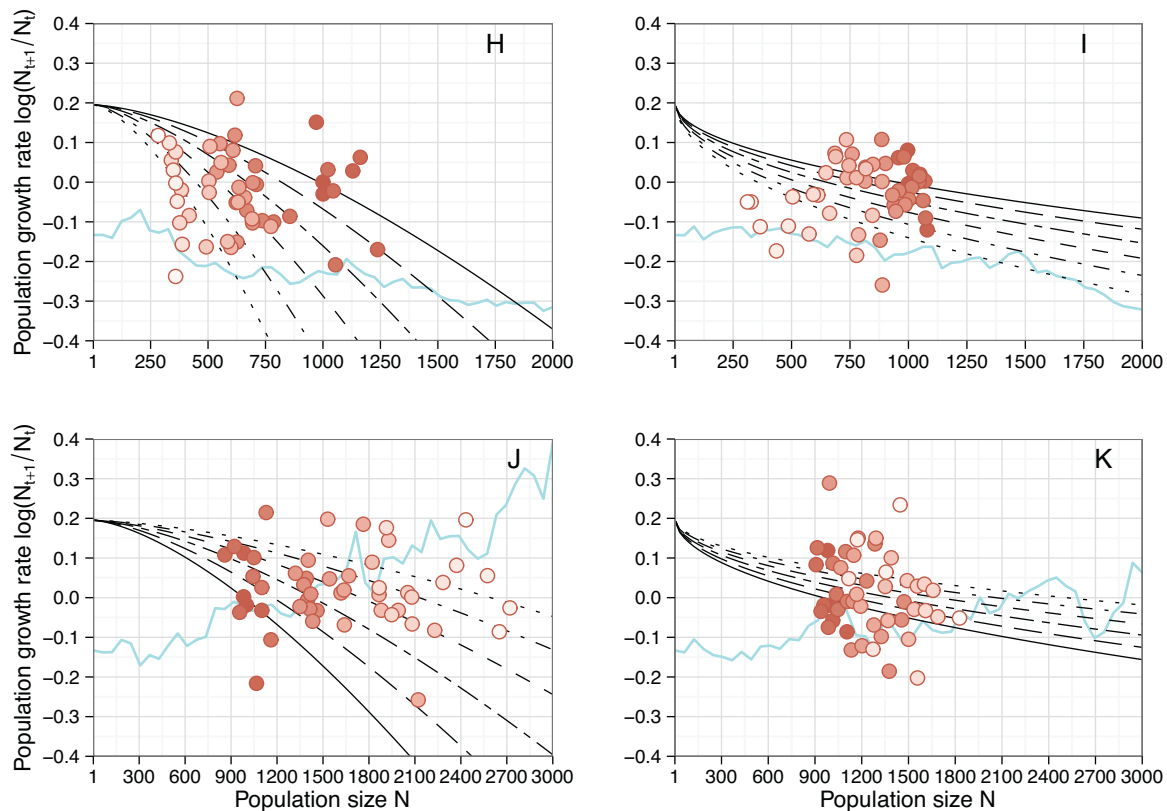


**Fig. 3.** Information contained in time series data of a gradual change in  $K$ . The points are sample population growth rates,  $\Delta X$ , gradually changing from  $K(0)$  (●) to  $K(49)$  (○). The lines are the stochastic growth rate at  $t=0$  (solid) and every 10th time step down to  $t=49$  (dotted). In the background are schematic illustrations of the population time series with the arithmetic scale (range 0–2900) on the y-axis and time (range 1–50) on the x-axis. In H and I,  $\kappa = 0.98$ . In J and K,  $\kappa = 1.02$ . In H and J,  $\theta = 1.5$ . In I and K,  $\theta = 0.5$ . In all cases  $r_1 = 0.2$ ,  $K = 1000$  and  $\sigma_e^2 = 0.01$ .

## 2.4. Simulation studies

For each of the three different temporal change scenarios examined, a few simulated examples are chosen to make some general remarks about the ability to estimate these changes. A summary of the different cases is found in Table 1. Cases A–C consider step-wise change in growth rate,  $r_1$ . In order to study what information is contained in the time series about the growth rate, the initial population size is either set to be a small number of individuals (20) or equal to  $K$  (1000). However, since there is a step-wise change in  $r_1$ , different accuracies of the estimates of this change  $\rho$  might be obtained depending on the population sizes after the change. Therefore, in Case C, the population size right after the change in  $r_1$  is artificially reduced down to 20. The reduction is done in order to get a second ‘growth phase’ giving information about  $r_1$  after the change and thus  $\rho$ . Cases A–C are illustrated in Fig. 1. The effect that sampling error and the number of observations have on the estimates are also investigated. Combining two different magnitudes of sampling error (none or equal to the environmental variance) and five different sample sizes, 200 runs have been simulated to obtain point estimates distributions, illustrated by violin plots (Hintze and Nelson, 1998). To separate the effect of sample size from the effect of populations having either small initial population size or starting around carrying capacity, all runs are simulated with the same length and point of change  $s$  as they are in Fig. 1. For the estimation, the same number of observations before and after  $s$  is chosen to constitute the sample, e.g.  $s - 5, s - 4, \dots, s - 1, s, s + 1, \dots, s + 4$  is a sample of ten observations. (An illustration of the sample sizes for Case A is presented in Fig. B.8 in B.)

Cases D–G consider step-wise changes in carrying capacity,  $K$ . The differences between cases D–G are the direction of the change in carrying capacity (increase or decrease) and the shape and strength of density regulation determined by  $\theta$ . Cases D–G are illustrated in Fig. 2. Effects of sample size and sampling error are investigated in the same manner as in Case A–C, however the number of observations before  $s$  is fixed at five, while the number of observations from  $s$  and onwards increases, e.g.  $s - 5, \dots, s - 1, s, s + 1, \dots, s + 4$  and  $s - 5, \dots, s - 1, s, s + 1, \dots, s + 14$  are samples with ten and 20 observations, respectively. The division of observations around  $s$  is to illustrate a scenario where the effect of an anthropogenic disturbance is to be measured in a species, but the researchers have a minimum of observations before the change (e.g. construction, regulation, deforestation) occur and then continue to monitor the species subsequently.

Finally, Cases H–K examine gradual changes in  $K$ . Both increasing and decreasing trends are considered and the same strengths of density regulation are used as for the step-wise changes in  $K$ . Cases H–K are illustrated in Fig. 3. In addition to these four cases, the effect of sample size, magnitude of change (% annually), direction (increasing or decreasing) and two different prior distributions on the mean return time to equilibrium  $T_R = \gamma^{-1}$  are considered, by calculating the proportion of estimates (out of 500 for each combination) that indicates a significant change in carrying capacity determined by whether or not zero is in the credible interval of  $\ln K$  for all the different combinations.

## Grey Heron introductory example

The following example highlights some of the main points of this study using a Grey Heron population in southern Britain. The data set is available from the Global Population Dynamics Database (NERC, 2010) and has previously been studied assuming stationary dynamics (Lande et al., 2002; Brook et al., 2006). Looking at the plotted time series (Fig. 4), a linearized model with gradually changing mean is fitted to the data (Sections 2.2 and 2.3). The linearized model provide a good approximation of the theta-logistic model as there are no observations of the population at small abundances, which are critical to obtain good estimates of the growth rate (Section 3.1 and Fig. 1). The estimated change in carrying capacity is an increase of 0.56% annually, and the 95% credible interval of (0.056, 1.04) indicates a significant increase. The length of the time series indicates that the significant change in carrying capacity is reliable (Section 3.3 and Fig. 7). The estimated strength of density regulation is 0.21, which is similar to the result of Lande et al. (2002) and corresponds to a mean return time to equilibrium of roughly five years. However, if there was prior belief that the strength of density regulation was weaker, e.g. close to 0.1, the 95% credible interval for the change in carrying capacity would increase to (−0.24, 1.33), i.e. there would be no significant evidence of a gradual increase in carrying capacity. The additional results for this example is found in Appendix C and all the code in Appendix J.

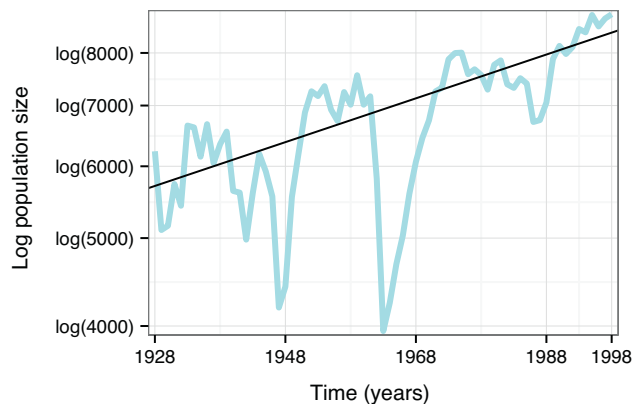


**Fig. 4.** Population counts of Grey Heron in southern Britain (blue line). A linear model with gradually changing carrying capacity (black line) is fitted to the data and the estimated parameters are  $\gamma=0.21$ ,  $K=5710$ ,  $\kappa=1.0056$ ,  $\sigma_e^2=0.011$  and  $\tau^2=0.00011$ . (For interpretation of the references to colour in this figure legend, the reader is referred to the web version of this article.)

## 3. Results

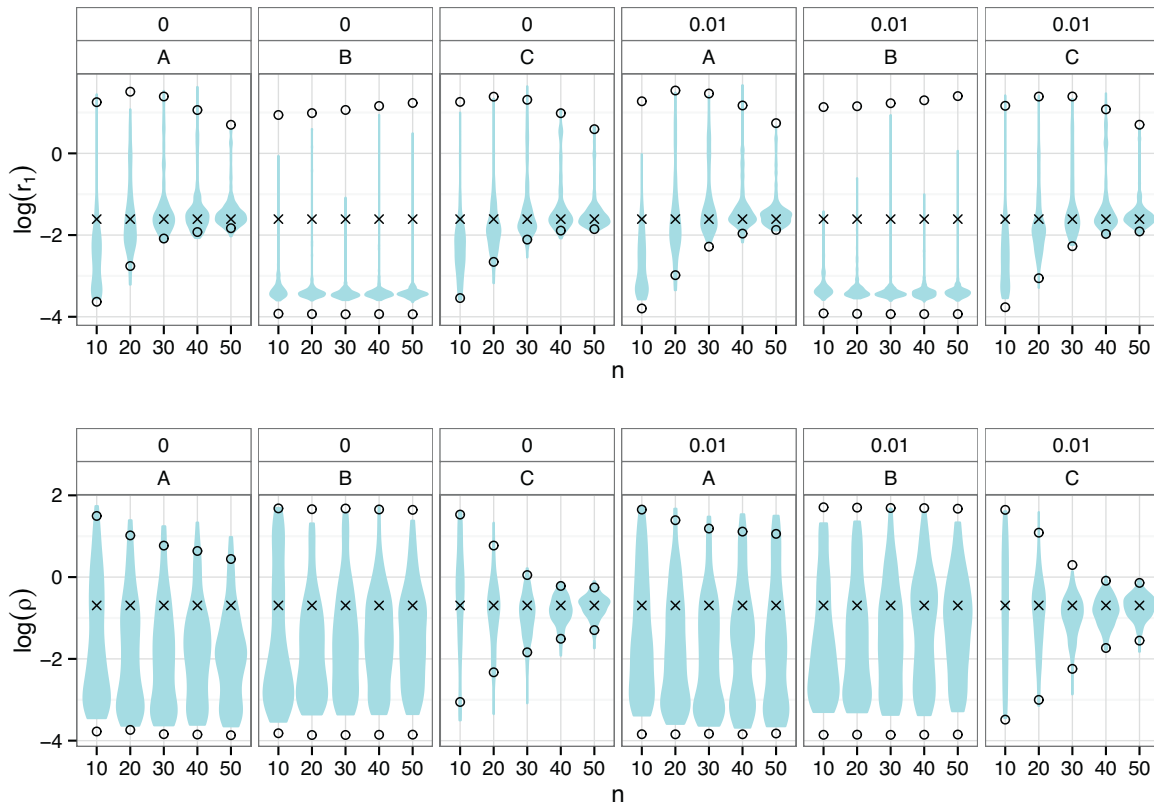
### 3.1. Estimation of temporal change in growth rate

Table 2 summarizes the point estimates and credible intervals of  $r_1$  and  $\rho$  (and the other parameters) for the three cases of step-wise change in growth rate that are illustrated in Fig. 1. In Case A, the

**Table 2**

Maximum posterior estimates (MAP) and credible intervals from the analysis of the three sample cases of step-wise changes in  $r_1$ , illustrated in Fig. 1. In A and C the initial population size is  $N_0=20$ . In B the initial population size is  $N_0=K$ . In C the population size is reduced to 20 at  $t=s$ , i.e. at the point where the growth rate is halved. The true parameter values are  $r_1=0.2$ ,  $\rho=0.5$ ,  $\theta=1.5$ ,  $K=1000$ ,  $\sigma_e^2=0.01$  and  $\tau^2=0.01$ .

Case	$r_1$		$\rho$		$\theta$		$K$		$\sigma_e^2$		$\tau^2$	
	MAP	Cred.int.	MAP	Cred.int.	MAP	Cred.int.	MAP	Cred.int.	MAP	Cred.int.	MAP	Cred.int.
A	0.204	0.153, 1.942	0.370	0.021, 2.308	4.589	0.032, 7.003	972.8	851.2, 7233.5	0.019	0.003, 0.032	0.008	0.000, 0.018
B	0.033	0.019, 4.362	0.101	0.021, 4.993	0.033	0.019, 5.594	1060.5	5.2, 16191.2	0.012	0.001, 0.030	0.025	0.007, 0.040
C	0.262	0.166, 2.817	0.432	0.115, 0.759	0.568	0.021, 3.452	1610.5	1005.5, 19743.5	0.024	0.003, 0.040	0.007	0.000, 0.019



**Fig. 5.** Violin plots of  $\log r_1$  (top row) and  $\log \rho$  (bottom row), representing step-wise change in  $r_1$ , for different sample sizes and sampling error. The violins are log values of the maximum a posteriori estimates from 200 time series for each combination of sample size  $n$  and sampling variance  $\tau^2$ . The points are the mean upper and lower 95% credible intervals of the posterior distributions ( $\circ$ ). The crosses are the true values ( $\times$ ). The parameter values are  $r_1 = 0.2$ ,  $\rho = 0.5$ ,  $\theta = 1.5$ ,  $K = 1000$  and  $\sigma_e^2 = 0.01$ . The change in growth rate occurs at  $s = 26$  when  $n = 50$ . When  $n = 40$ , the five first and five last observations are removed and so on. The columns with '0' and '0.01' indicate the value of  $\tau^2$ , while A–C are the cases described in the text and illustrated in Fig. 1.

estimate of  $r_1$  is accurate which is reasonable since the population is observed from a small population size up to carrying capacity. The point estimate of  $\rho$  indicate a reduction in growth rate  $\rho < 1$  although the credible interval is wide and include 1, so the possibility of no change cannot be rejected. When the population is observed starting at carrying capacity, Case B, the estimates of both  $r_1$  and  $\rho$  show that the data contain little information about these parameters and the resulting posterior distributions are close to their respective vague priors. As the ‘ideal’ situation for observing change in growth rate, where there are two separate growth phases, before and after the change, Case C gives us the most accurate estimates of both  $r_1$  and  $\rho$ .

To get a more general overview, Fig. 5 illustrates the violin plots of  $\log r_1$  and  $\log \rho$ , with and without sampling error for different sample sizes. When the sample size increases, the estimates are expected to improve, but this is only the case if the additional observations cover a growth phase. Therefore, the estimates of  $r_1$  improves for Cases A and C, while reasonable estimates of  $\rho$  is only obtained in Case C, where the population is ‘reset’ to 20 individuals after the change occurs at time  $s$ . When sampling error  $\tau^2$  are introduced in the simulations, the estimates of  $r_1$  and  $\rho$  become less precise. The increased uncertainty in parameter estimates due to sampling error is most apparent for Case C, which had the best estimates of  $r_1$  and  $\rho$ , and the estimate of  $r_1$  in Case A. The other estimates for Case A and B do not change much with sampling error, but these were very inaccurate even without sampling error. The violin plots for the other parameters in Case A–C are found in Appendix D (Fig. D.9), along with the parameter estimates of the simulations in Fig. 1 when there is no sampling error (Table D.6).

### 3.2. Estimation of step-wise change in carrying capacity

The parameter estimates and credible intervals for the four cases of step-wise change in carrying capacity (D–G, Fig. 2), using the linear model with different priors on  $\beta$ , are summarized in Table 3. For the reduction in carrying capacity, the point estimates of  $\kappa$  are accurate, while the  $\kappa$ ’s are underestimated when carrying capacity increases. The credible intervals indicate a significant reduction in carrying capacity in all cases where an actual reduction is simulated, except E2 where the prior on  $\beta$  is close to the true value of 0.1. For the step-wise increase simulations, none of the cases are significant except F2 where the prior is close to the true value of 0.3. Comparing the columns for  $\gamma$  and  $\kappa$ , illustrates that the higher the strength of density regulation, the shorter the credible intervals of  $\kappa$ .

The violin plots in Fig. 6 further illustrate the differences between the two assigned prior distributions. For the step-wise decrease (case D), the credible intervals indicate, on average, a significant decline in carrying capacity with 20 observations when using a strong prior on the strength of density regulation (lower left corner, Fig. 6). Using a vague prior on  $\beta$  when estimating the step-wise decrease (upper left corner, Fig. 6), a significant decline in carrying capacity is indicated with 40 observations, although with a much wider credible interval compared to the same case with a strong prior on  $\beta$ . In contrast, it is significantly more difficult to detect the same magnitude of change in the opposite direction, that is, an increase in carrying capacity (Case F). With a vague prior on  $\beta$ , there is no guarantee of concluding that there is a significant change in  $K$  even with 50 observations, but using a strong prior on  $\beta$ , a significant increase is detectable with 30 observations.

**Table 3**

Posterior means and credible intervals from the analysis of the four sample cases of step-wise changes in  $K$ , illustrated in Fig. 2. In D and E,  $\kappa = 0.5$ . In F and G,  $\kappa = 1.5$ . In D and F,  $\theta = 1.5$ . In E and G,  $\theta = 0.5$ . The numbering of the cases indicates the prior distribution on  $\log \beta$  used: (1)  $N(0, 5)$  (2)  $N(\ln \gamma, 0.01)$ . The other parameter values are  $r_1 = 0.2$ ,  $K = 1000$ ,  $\sigma_e^2 = 0.01$  and  $\tau^2 = 0.01$ .

Case	$\gamma$	$K$		$\kappa$		$\sigma_e^2$		$\tau^2$		
		Mean	Cred.int.	Mean	Cred.int.	Mean	Cred.int.	Mean	Cred.int.	
D1	0.514	0.166, 1.072	951.0	798.1, 1140.1	0.556	0.440, 0.736	0.047	0.026, 0.078	0.000	0.000, 0.001
D2	0.306	0.250, 0.370	967.1	756.5, 1209.3	0.573	0.411, 0.801	0.040	0.026, 0.059	0.000	0.000, 0.001
E1	0.281	0.099, 0.553	1184.8	903.9, 1497.2	0.543	0.386, 0.815	0.036	0.022, 0.055	0.000	0.000, 0.001
E2	0.101	0.083, 0.122	1194.2	775.6, 1748.4	0.598	0.341, 1.055	0.021	0.009, 0.047	0.006	0.001, 0.014
F1	0.158	0.027, 0.435	987.1	804.0, 1236.2	1.335	0.952, 1.733	0.008	0.002, 0.023	0.009	0.004, 0.017
F2	0.297	0.243, 0.359	964.6	845.1, 1101.6	1.372	1.134, 1.654	0.012	0.004, 0.026	0.008	0.003, 0.016
G1	0.391	0.158, 0.719	934.6	734.3, 1137.6	1.171	0.870, 1.591	0.045	0.027, 0.069	0.000	0.000, 0.001
G2	0.102	0.083, 0.123	1059.9	648.5, 1605.2	1.174	0.632, 2.213	0.026	0.011, 0.058	0.006	0.001, 0.017

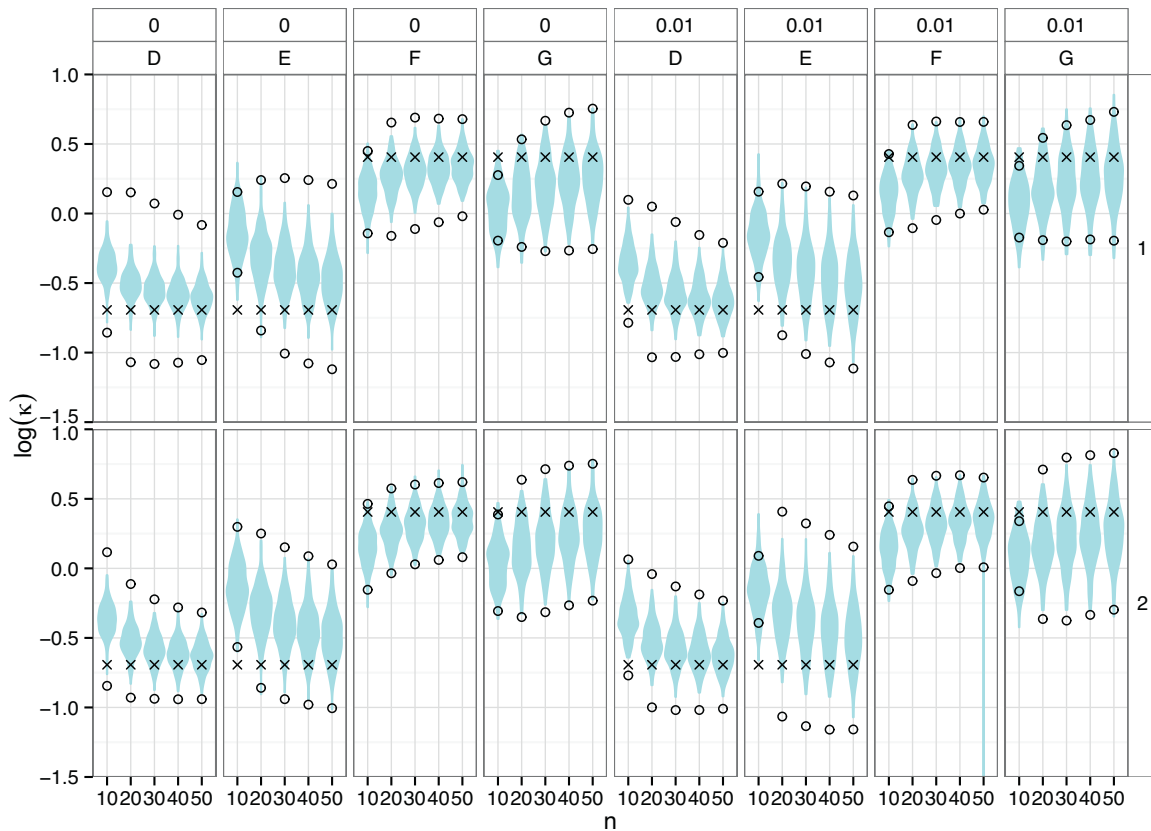


**Fig. 6.** Violin plots of  $\log \kappa$ , representing step-wise change in  $K$ , for different sample sizes, sampling error and prior distribution on  $\beta$ . The violins are log values of the mean posterior distribution from 200 time series for each combination of sample size  $n$ , sampling variance  $\tau^2$  and prior  $\pi(\beta)$ . The points are the mean upper and lower 95% credible intervals of the posterior distributions ( $\circ$ ). The crosses are the true values ( $\times$ ). The parameter values are  $r_1 = 0.2$ ,  $K = 1000$  and  $\sigma_e^2 = 0.01$ . The change in carrying capacity occurs at  $s = 6$  for all values of  $n$ . The columns with '0' and '0.01' indicate the value of  $\tau^2$ , D–G are the cases described in the text and illustrated in Fig. 2, while in row 1  $\log \beta \sim N(0, 20)$  and row 2  $\log \beta \sim N(\ln \gamma, 0.01)$ .

The reason why it is more difficult to observe an increase can be seen by comparing the difference between the growth curves for Case D and F in Fig. 2. If the population is around the initial carrying capacity  $K$  which is then reduced by  $\kappa$ , the expected population growth rate is  $-0.4$  in the decreasing case and only  $0.1$  in the increasing case. Species with strong density dependence (in this case  $\theta = 1.5$ ) will have a much more distinct response to step-wise decrease in carrying capacity than increase. Species with weaker density dependence, such as  $\theta = 0.5$  in Fig. 2 (Case E and G), have an expected population growth rate of approximately  $-0.1$ , and  $0.05$  by a decrease or increase in carrying capacity, respectively. Fig. 6 illustrates that it is not expected to find a significant step-wise change in either direction, even with 50 observations, with a long return time to equilibrium ( $T_R = 1/\gamma = 10$ ). The

average credible intervals are slightly shorter for a reduction in  $K$  with a strong prior on  $\gamma$ .

A counter-intuitive result in Fig. 6 is the shorter mean credible intervals for step-wise decrease in carrying capacity with short return time to equilibrium and sampling error (D1) compared to no sampling error. This is a consequence of the estimates of  $\gamma$  in these two cases. In D1 with no sampling error, the  $\gamma$  is slightly underestimated, while there is a tendency to over-estimation when there are sampling error and much wider credible intervals. In addition, the estimates of the sampling error in the latter case are very uncertain. Thus, more of the additional fluctuations due to sampling error is now attributed to rapid fluctuations around carrying capacity. The respective violin plots of the other parameter estimates are found in Appendix E (Figs. E.10 and E.11).

**Table 4**

Posterior means and credible intervals from the analysis of the four sample cases of gradual changes in  $K$ , illustrated in Fig. 3. In H and I,  $\kappa = 0.98$ . In J and K,  $\kappa = 1.02$ . In H and J,  $\theta = 1.5$ . In I and K,  $\theta = 0.5$ . The numbering of the cases indicates the prior distribution on  $\log \beta$  used: (1)  $N(0, 5)$  (2)  $N(\ln \gamma, 0.01)$ . The other parameter values are  $r_1 = 0.2$ ,  $K = 1000$ ,  $\sigma_e^2 = 0.01$  and  $\tau^2 = 0.01$ .

Case	$\gamma$	$K$		$\kappa$		$\sigma_e^2$		$\tau^2$		
		Mean	Cred.int	Mean	Cred.int	Mean	Cred.int	Mean	Cred.int	
H1	0.486	0.203, 0.891	1126.6	925.0, 1372.3	0.977	0.970, 0.983	0.031	0.019, 0.051	0.000	0.000, 0.001
H2	0.308	0.252, 0.372	1124.9	864.2, 1441.5	0.977	0.968, 0.986	0.028	0.018, 0.040	0.000	0.000, 0.001
I1	0.269	0.088, 0.545	1284.9	919.5, 1751.1	0.980	0.969, 0.990	0.036	0.021, 0.062	0.000	0.000, 0.001
I2	0.101	0.082, 0.122	1294.4	782.4, 1954.4	0.978	0.963, 0.993	0.017	0.006, 0.039	0.008	0.002, 0.018
J1	0.329	0.030, 1.223	901.5	810.9, 1003.9	1.023	1.019, 1.026	0.001	0.000, 0.008	0.021	0.009, 0.053
J2	0.301	0.246, 0.363	903.8	803.7, 1024.2	1.023	1.018, 1.027	0.001	0.000, 0.006	0.034	0.009, 0.127
K1	0.714	0.315, 1.300	1000.6	858.8, 1153.2	1.010	1.005, 1.016	0.035	0.019, 0.059	0.000	0.000, 0.001
K2	0.102	0.083, 0.124	1084.8	711.7, 1544.2	1.010	0.997, 1.024	0.012	0.004, 0.030	0.007	0.002, 0.020

### 3.3. Estimation of gradual change in carrying capacity

**Table 4** summarizes the parameter estimates for the four gradual changes in carrying capacity illustrated in Fig. 3. Although the two different priors on  $\beta$  (method 1 and 2) have little effect on the estimated annual change in carrying capacity  $\kappa$  the differences observed are similar to those of the step-wise change. In Case K1 (gradual increase, long return time, vague prior), the strength of density dependence is over-estimated and although estimated trend in carrying capacity is smaller than the true change, the credible interval is slightly above one (no trend) so a significant change in carrying capacity can be concluded. Choosing a prior that is close

to the true value, i.e. a much longer return time to equilibrium (K2), the point estimates does not change much, but the credible interval becomes wider (also the case for the initial carrying capacity  $K$ ) and the hypothesis that there is no trend would not be rejected in this case. The over-estimation of  $\gamma$  is also present for the other cases, but the changes in credible interval for  $\kappa$  are smaller.

How often a trend will be inferred from different sample sizes and magnitudes of change is quantified in Fig. 7 by illustrating the proportion of credible intervals of  $\ln \kappa$  that does not include zero, under different magnitudes of either increasing, decreasing or no change in carrying capacity. When the return time is 3 years (top row) with a vague prior on  $\gamma$ , changes are significant almost

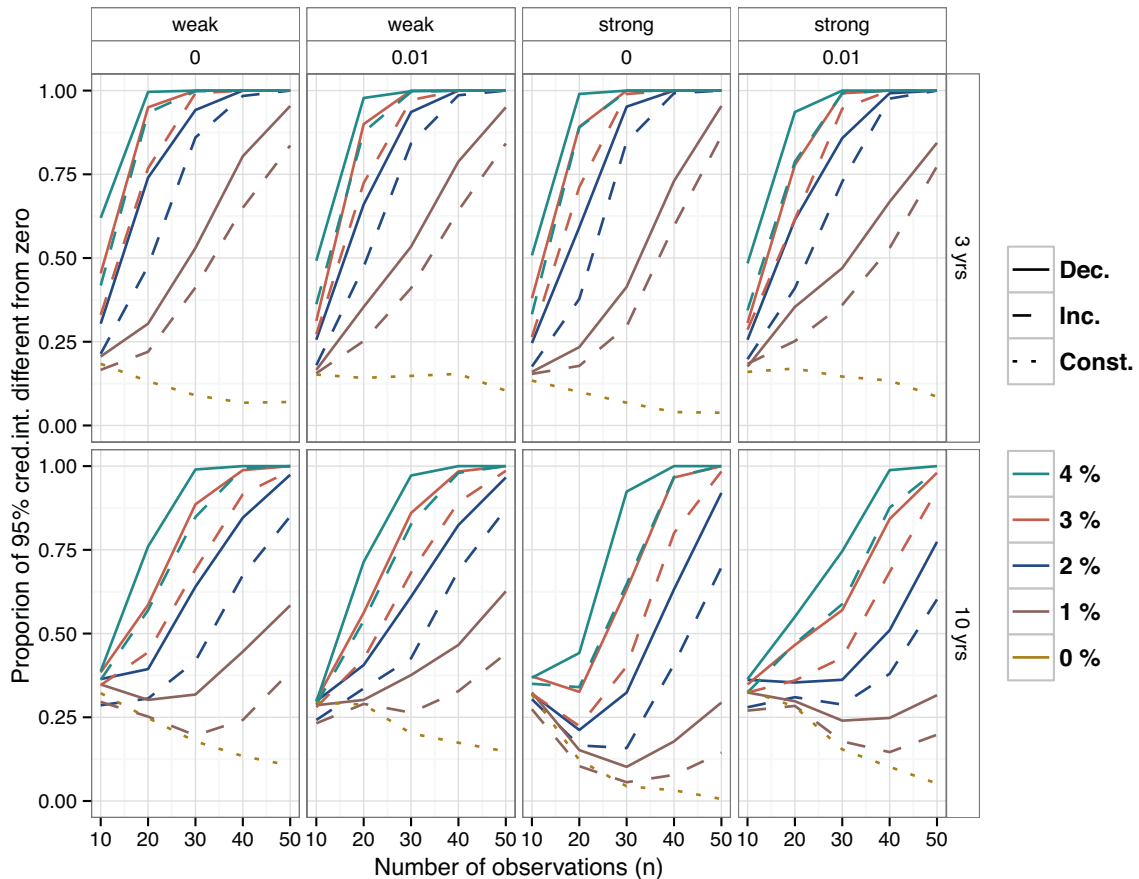


**Fig. 7.** Proportion 95% credible intervals for  $\log \kappa$  that does not include zero, i.e. indicate significant trends in carrying capacity. In the first two columns a 'vague' prior on the strength of density dependence,  $\pi(\log \gamma) \sim N(0, 5)$  is used, while in the last two columns used  $\pi(\log \gamma) \sim N(\ln \gamma, 0.01)$  ('strong'). In the first row,  $\gamma = 0.3$ , while  $\gamma = 0.1$  in the second row. The other parameter values are  $K = 1000$ ,  $\sigma_e^2 = 0.01$  and the sampling error,  $\tau^2$ , is either zero or 0.01. The proportions are out of 500 simulations for each combination.

certainly after 30 observations, when the true changes are 3% or 4%. An annual decline of 3% and 4% over 30 years corresponds to a reduction down to 40% and 30% of the initial value, respectively, which is a considerable reduction of a species' carrying capacity. Applying the stronger prior on the strength of density regulation, the proportions are barely changed compared to the results using a vague prior on  $\gamma$ . There is a significant difference between the proportions of a decreasing and increasing trend, roughly 10–15% points lower for increasing trends in some cases, so an extra ten years of observations is needed to achieve similar proportions for increasing as for decreasing trends.

For species with long return time to equilibrium (10 years, bottom row), a decline of 2% annually will be detected in 60% of the simulations after 30 observations, using a vague prior on the strength of density dependence, but this proportion is reduced to 45% of the simulations when the strong prior on  $\gamma$  is applied. The reason why the proportion is greater, using a vague prior on  $\gamma$ , is that the strength of density dependence is over-estimated and the credible intervals of the gradual change in carrying capacity  $\kappa$  becomes more narrow and more often do not include  $\kappa=1$  (no change). As in the case of the short return time to equilibrium, a gradual increase in carrying capacity is considerably more difficult to detect than a decrease.

#### 4. Discussion

Time series of population counts or density are the most basic data available to ecologists, but acquiring fairly accurate sample points can be both expensive and time consuming. The models used to describe population fluctuations rely on accuracy of parameter estimates, which are influenced by the uncertainty in the sampling procedure (Bjørnstad and Grenfell, 2001; Lebreton and Gimenez, 2013). Several methods are available to estimate density dependency while accounting for sampling error (Staudenmayer and Buonaccorsi, 2005; Dennis et al., 2006; Wang, 2007; Ives et al., 2010; Pedersen et al., 2011; Dennis and Ponciano, 2014) and several of those provide tests for density dependence (see Herrando-Pérez et al. (2012) for a summary). This work assume that the populations are density dependent and that trends in the population fluctuations are either due to a population growth phase, from small abundances up to carrying capacity, or caused by deterministic changes in the parameters, and not due to trends caused by density independent growth (Humbert et al., 2009). Time series with trends are usually de-trended, e.g. by subtracting a regression line from the data, before analyzing the 'stationary' dynamics. However, de-trending can give very different dynamic models compared to assuming no trend and researchers must take this into account when making inferences (Turchin, 2003).

Within a Bayesian framework, two models have been fitted using different estimation approaches to study changes in dynamical parameters. Estimating the parameters of a stationary theta-logistic model with sampling error have been studied extensively by Wang (2007), Pedersen et al. (2011) and shown to yield reasonable results for simulated examples. The theta-logistic model has been used in order to study step-wise changes in growth rate  $r_1$ . Unless the time series data contains observations of abundances well below carrying capacity, accurate estimates of  $r_1$  are difficult to obtain (Fig. 1). To reveal a change in the growth rate with a high degree of credibility will require data from periods with low abundance both before and after the change (Fig. 5). Studying temporal changes in the growth parameter is better done using demographic data such as number of offspring and adult survival, rather than time series of population counts (Margalida et al., 2014).

Because of the inaccurate estimates of  $r_1$  in the absence of a growth phase in population time series, a linearization of the

theta-logistic model around log carrying capacity is a reasonable approximation of the population dynamics if the fluctuations around  $\ln K$  are moderate (Solbu et al., 2013). Although there are large uncertainties in the estimates (Fig. 7), this is due to a lack of observations and not a shortcoming of the approximation. Temporal changes in carrying capacity were studied using data without a growth phase to illustrate a situation where there has not been any long term study of the population before the changes (Figs. 2 and 3). If the data should include a growth phase first, a non-linear model should be fitted, but 10–20 observations could then potentially include no information about the carrying capacity, which is the parameter of interest in these examples. Naturally, if the true carrying capacity is small, e.g. around 100, a non-linear model would also be preferred since the fluctuations would then be closer to small abundances which gives information about  $r_1$ .

The use of INLA to fit the parameters of the linear Ornstein–Uhlenbeck (OU) model, is a more novel approach in ecology. Dennis and Ponciano (2014) fitted the OU model to data with unequal time intervals, using restricted maximum likelihood estimation (REML). The OU model in INLA can also handle data series with unequal time intervals. The REML approach is slower computationally, which can be an issue when studying multiple combinations of sample size and parameter values. Comparing parameter estimates of the case studies in Dennis and Ponciano (2014) to estimates using INLA show close similarities, but parameters that are difficult to estimate such as the strength of density dependence and sampling error can differ greatly (see Table I.9 in Appendix I).

The strong prior distributions on the strength of density dependence  $\gamma$  is an attempt to deal with the inaccurate estimates of this parameter. Although experts might not think in terms of 'mean return time to equilibrium', its reciprocal, the strength of density regulation, is approximately equal to the growth rate at small population sizes for  $\theta$  around one. The growth rate might be an easier parameter to obtain prior information about, from demographic data not necessarily collected across all years. Nevertheless, even when applying strong prior, the results did not unconditionally improve the ability to detect that a change was occurring. The lack of improvement was particularly the case when considering changes in populations with long return time to equilibrium, or weak density dependence. Without strong priors on  $\gamma$ , the strength of density dependence were usually over-estimated and it seems to be more profound under the assumption of a trend in carrying capacity. Having perfect knowledge about the population dynamics would give the most moderate prospect of concluding in favor of a trend. A conservative approach could be reasonable in cases where an increase over time was interpreted as a recovering population, but equally hazardous if a population decline was observed.

When a strong prior on  $\gamma$  implies a long return time to equilibrium, an assumption of temporal change in carrying capacity is more difficult to estimate accurately because more of the observed fluctuations in population size is attributed to the weak density regulation instead of deterministic changes in carrying capacity. In order to determine that fluctuations in abundance are not due to weak density regulation, but consequence of change in carrying capacity, the population has to be monitored over a time span that exceeds the mean return time to equilibrium by several magnitudes. Using a vague prior, the conclusion on a trend will occur more often, even when there are none, e.g.  $\approx 20\%$  of the time with 30 observation when  $\gamma = 0.1$ , but the other population dynamical parameters could potentially be very inaccurate. Although these results might be discouraging in some aspects, it is important to know the limits in statistical power and accept the potentially large uncertainty in the inference and apply the precautionary principle when determining the effect of human interference with populations.

## Acknowledgements

This work was supported by the European Research Council (ERC-2010-AdG 268562) and the Norwegian University of Science and Technology. The work of OHD was possible due to financial support from the Norwegian Institute for Nature Research. We thank two anonymous reviewers for constructive comments and suggestions that helped improve the manuscript.

## Appendix A. Theory

Given a diffusion process

$$dN_t = \mu_N(n)dt + \sqrt{\nu_N(n)}dB_t$$

where  $\mu_N(n) = r_0 n [1 - (n/K)^\theta]$  and  $\nu_N(n) = \sigma_e^2 n^2 + \sigma_d^2 n$ . A monotone transformation  $X = \ln(N)$  is then a diffusion process (Karlin and Taylor, 1981)

$$dX_t = \mu_X(x)dt + \sqrt{\nu_X(x)}dB_t$$

where  $\mu_X(x) = g'(n)\mu_N(n) + \frac{1}{2}g''(n)\nu_N(n)$  and  $\nu_X(x) = [g'(n)]^2\nu_N(n)$ . Using these expressions we get  $\mu_X(x) = r_0[1 - (e^x/K)^\theta] - (\sigma_e^2 + \sigma_d^2/e^x)/2$  and  $\nu_X(x) = \sigma_e^2 + \sigma_d^2/e^x$ . Linearizing  $\mu_X(x)$  around  $\ln K$  we get the approximation  $\mu_X^*(x) \approx \beta(\alpha - x)$ , where  $\alpha = \ln K - (\sigma_e^2 + \sigma_d^2/K)/(2r_0\theta + \sigma_d^2/K)$  and  $\beta = r_0\theta + \sigma_d^2/(2K)$ . Thus, the transformed diffusion process is

$$dX_t = \beta(\alpha - X_t)dt + \sqrt{\sigma_e^2 + \sigma_d^2/e^{-X_t}}dB_t.$$

The output from INLA provides estimates of the following parameters  $(\alpha_0, \alpha_1, \beta, \varepsilon, \zeta)$ , where  $\varepsilon = [\sigma_e^2/(2\beta)]^{-1}$  and  $\zeta = 1/\tau^2$ . If demographic variance is estimated separately from data on the individual level, this estimate can be used to adjust the estimated environmental variance by the following equation

$$\hat{\sigma}_e^2 = \hat{\varepsilon}^{-1} 2\hat{\beta} - \hat{\sigma}_d^2 \frac{\sum_{i=1}^n \exp\{-\hat{X}_i\}(1 - \exp\{-2\hat{\beta}\delta_i\})}{\sum_{i=1}^n (1 - \exp\{-2\hat{\beta}\delta_i\})}.$$

If the observations are equidistant, this simplifies to  $\hat{\sigma}_e^2 = \hat{\varepsilon}^{-1} 2\hat{\beta} - \hat{\sigma}_d^2 \sum_{i=1}^n \exp\{-\hat{X}_i\}/n$ , so the environmental variance is reduced by an ‘average effect’ of demographic variance across the observed time frame. The change in carrying capacity is found as  $\hat{\kappa} = \exp\{\hat{\alpha}_1\}$ , while the initial carrying capacity is either

$$\hat{\kappa} = \exp \left\{ W \left( \frac{t_n \hat{\sigma}_d^2}{2\hat{\beta}[t_s + (t_n - t_s)\hat{\kappa}]} \exp \left\{ -\hat{\alpha}_0 - \frac{\hat{\sigma}_e^2}{2\hat{\beta}} \right\} \right) + \hat{\alpha}_0 + \frac{\hat{\sigma}_e^2}{2\hat{\beta}} \right\}$$

in case of a (single) step-wise change or

$$\hat{\kappa} = \exp \left\{ W \left( \frac{t_n \hat{\sigma}_d^2}{2\hat{\beta} \sum_{i=1}^n \hat{\kappa}^{t_{i-1}}} \exp \left\{ -\hat{\alpha}_0 - \frac{\hat{\sigma}_e^2}{2\hat{\beta}} \right\} \right) + \hat{\alpha}_0 + \frac{\hat{\sigma}_e^2}{2\hat{\beta}} \right\}$$

if the change is gradual. Then,  $\hat{\gamma} = \hat{\beta} - \hat{\sigma}_d^2/(2\bar{\kappa})$ , where  $\bar{\kappa} = \hat{\kappa}[t_s + (t_n - t_s)\hat{\kappa}]/t_n$  or  $\bar{\kappa} = \hat{\kappa} \sum_{t=1}^n \hat{\kappa}^{t-1}/t_n$  for step-wise or gradual change in carrying capacity, respectively. That is, we have replaced all instances of  $K$  in the denominators with the average value across the observed time span.

## Appendix B. Illustration

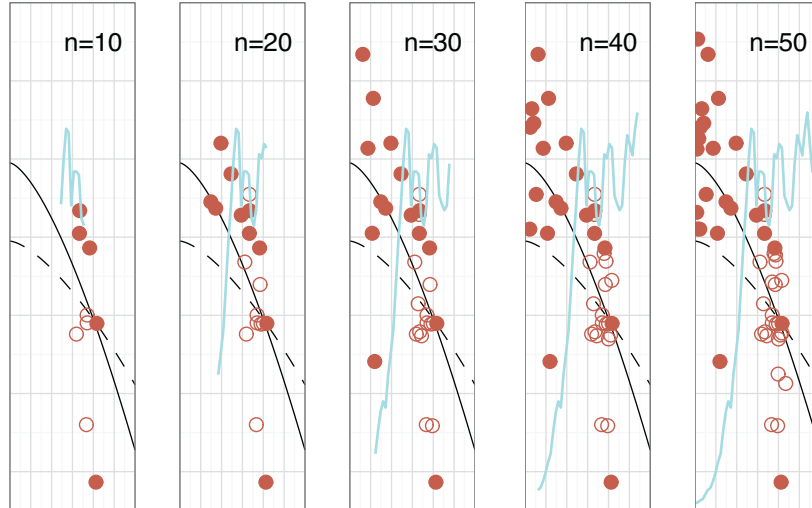


**Fig. B.8.** Illustration of how the sample sizes are chosen around the point of step-wise change at time  $s$  in order to separate the effect of sample size from the initial population size. This example is the step-wise change in  $r_1$  for a population who has an initial population size ( $N_0$ ) of 20, i.e. Case A in Fig. 1.

## Appendix C. Additional results for Grey Heron introductory example

**Table C.5**

Posterior means and credible intervals from the analysis of the Grey Heron data, illustrated in Fig. 4.

Case	$\gamma$		$K$		$\kappa$		$\sigma_e^2$		$\tau^2$	
	Mean	Cred.int	Mean	Cred.int	Mean	Cred.int	Mean	Cred.int	Mean	Cred.int
Weak prior	0.213	0.083, 0.394	5710.4	4658.0, 6858.0	1.006	1.001, 1.010	0.011	0.007, 0.015	0.000	0.000, 0.000
Strong prior <sup>a</sup>	0.102	0.084, 0.124	5981.4	4231.7, 8342.5	1.006	0.998, 1.013	0.010	0.007, 0.013	0.000	0.000, 0.000

<sup>a</sup> The strong prior in this case is  $\log \gamma \sim N(\log(0.1), 0.01)$  and only used as a illustration.

## Appendix D. Additional results for step-wise changes in growth rate

**Table D.6**

Maximum a posteriori estimates (MAP) and credible intervals from the analysis of the three sample cases of step-wise changes in  $r_1$ , illustrated in Fig. 1. In A and C the initial population size is  $N_0 = 20$ . In B the initial population size is  $N_0 = K$ . In C the population size is reduced to 20 at  $t=s$ , i.e. at the point where the growth rate is halved. The true parameter values are  $r_1 = 0.2$ ,  $\rho = 0.5$ ,  $\theta = 1.5$ ,  $K = 1000$ ,  $\sigma_e^2 = 0.01$  and  $\tau^2 = 0$ .

Case	$r_1$	$\rho$		$\theta$		$K$		$\sigma_e^2$		$\tau^2$		
		MAP	Cred.int.	MAP	Cred.int.	MAP	Cred.int.	MAP	Cred.int.	MAP	Cred.int.	
A	0.204	0.166, 0.488	0.296	0.022, 1.124	4.763	0.135, 7.096	975.0	903.4, 4255.5	0.007	0.003, 0.010	0.001	0.000, 0.002
B	0.035	0.020, 5.307	0.243	0.020, 4.504	0.039	0.020, 5.078	1091.5	9.2, 14827.6	0.013	0.006, 0.020	0.002	0.000, 0.006
C	0.313	0.218, 2.255	0.445	0.278, 0.602	0.311	0.024, 1.392	2029.0	1147.8, 18055.1	0.007	0.004, 0.011	0.001	0.000, 0.003

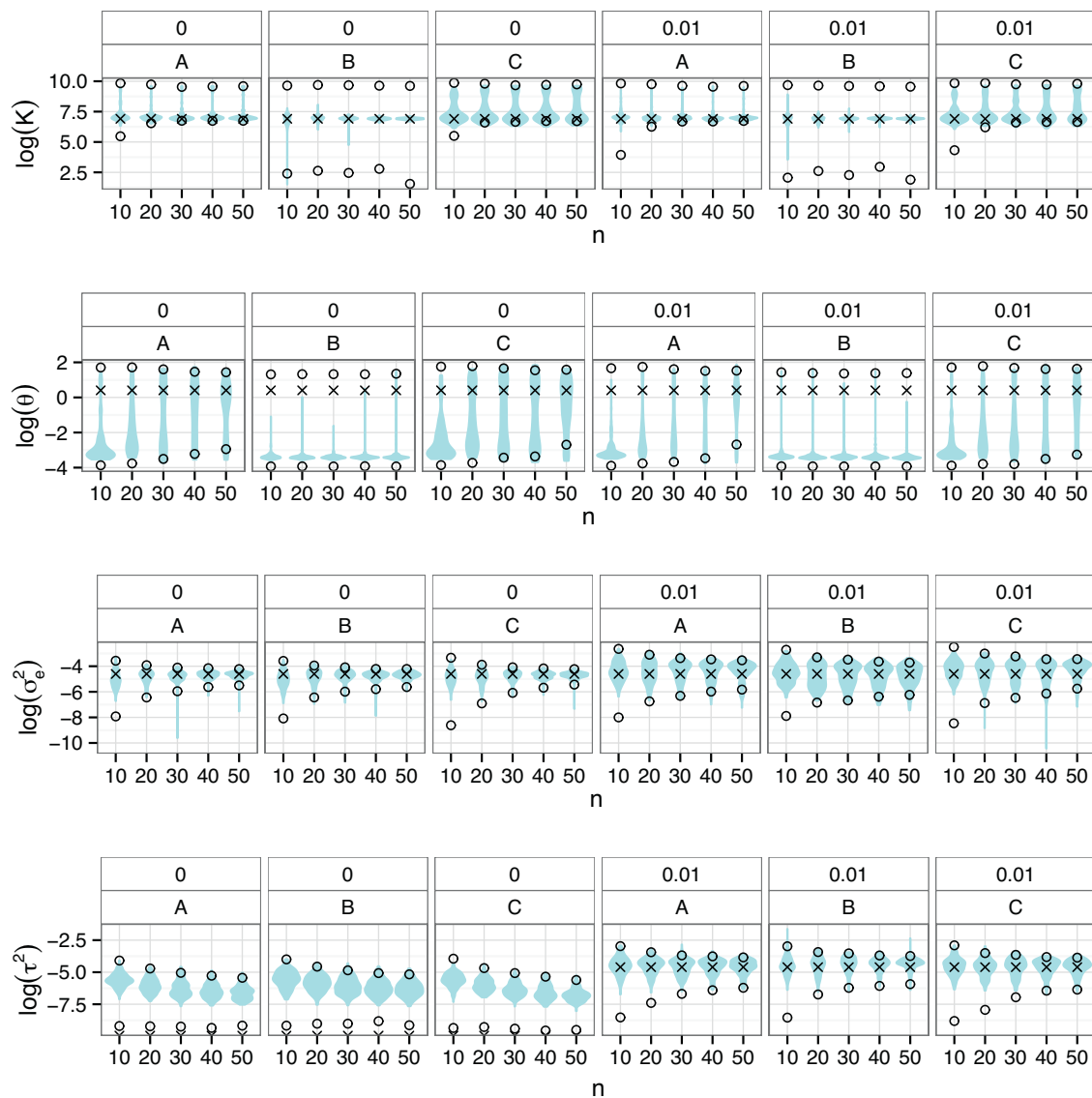


**Fig. D.9.** Violin plots of  $K$ ,  $\log \theta$ ,  $\log \sigma_e^2$  and  $\log \tau^2$ , for step-wise changes in  $r_1$ , for different sample sizes and sampling error. The violins are log values of the maximum a posteriori estimates from 200 time series for each combination of sample size  $n$  and sampling variance  $\tau^2$ . The points are the mean upper and lower 95% credible intervals of the posterior distributions ( $\circ$ ). The crosses are the true values ( $\times$ ). The parameter values are  $r_1 = 0.2$ ,  $\rho = 0.5$ ,  $\theta = 1.5$ ,  $K = 1000$  and  $\sigma_e^2 = 0.01$ . The change in growth rate occurs at  $s=26$  when  $n=50$ . When  $n=40$ , the five first and five last observations are removed and so on. The columns with '0' and '0.01' indicate the value of  $\tau^2$ , while A–C are the cases described in the text and illustrated in Fig. 1.

## Appendix E. Additional results for step-wise changes in carrying capacity

**Table E.7**

Posterior means and credible intervals from the analysis of the four sample cases of step-wise changes in  $K$ , illustrated in Fig. 2. In D and E,  $\kappa = 0.5$ . In F and G,  $\kappa = 1.5$ . In D and F,  $\theta = 1.5$ . In E and G,  $\theta = 0.5$ . The numbering of the cases indicates the prior distribution on  $\log \beta$  used: (1)  $N(0, 5)$  (2)  $N(\ln \gamma, 0.01)$ . The other parameter values are  $r_1 = 0.2$ ,  $K = 1000$ ,  $\sigma_e^2 = 0.01$  and  $\tau^2 = 0$ .

Case	$\gamma$	$K$		$\kappa$		$\sigma_e^2$		$\tau^2$		
		Mean	Cred.int.	Mean	Cred.int.	Mean	Cred.int.	Mean	Cred.int.	
D1	0.126	0.025, 0.306	995.5	718.1, 1469.8	0.594	0.385, 1.025	0.013	0.008, 0.020	0.000	0.000, 0.001
D2	0.293	0.241, 0.354	917.4	789.7, 1064.1	0.568	0.457, 0.707	0.016	0.010, 0.023	0.000	0.000, 0.001
E1	0.123	0.034, 0.265	1136.1	803.3, 1533.6	0.594	0.396, 1.012	0.013	0.008, 0.019	0.000	0.000, 0.001
E2	0.101	0.083, 0.122	1109.7	786.5, 1511.7	0.612	0.385, 0.977	0.012	0.008, 0.018	0.000	0.000, 0.001
F1	0.174	0.049, 0.370	988.8	795.5, 1274.3	1.361	0.959, 1.795	0.010	0.006, 0.015	0.000	0.000, 0.001
F2	0.296	0.243, 0.356	953.1	841.3, 1082.9	1.396	1.165, 1.670	0.011	0.007, 0.017	0.000	0.000, 0.001
G1	0.144	0.041, 0.305	951.5	718.6, 1248.2	1.147	0.773, 1.718	0.013	0.008, 0.020	0.000	0.000, 0.001
G2	0.101	0.083, 0.122	989.7	695.3, 1358.8	1.151	0.725, 1.826	0.012	0.008, 0.017	0.000	0.000, 0.001

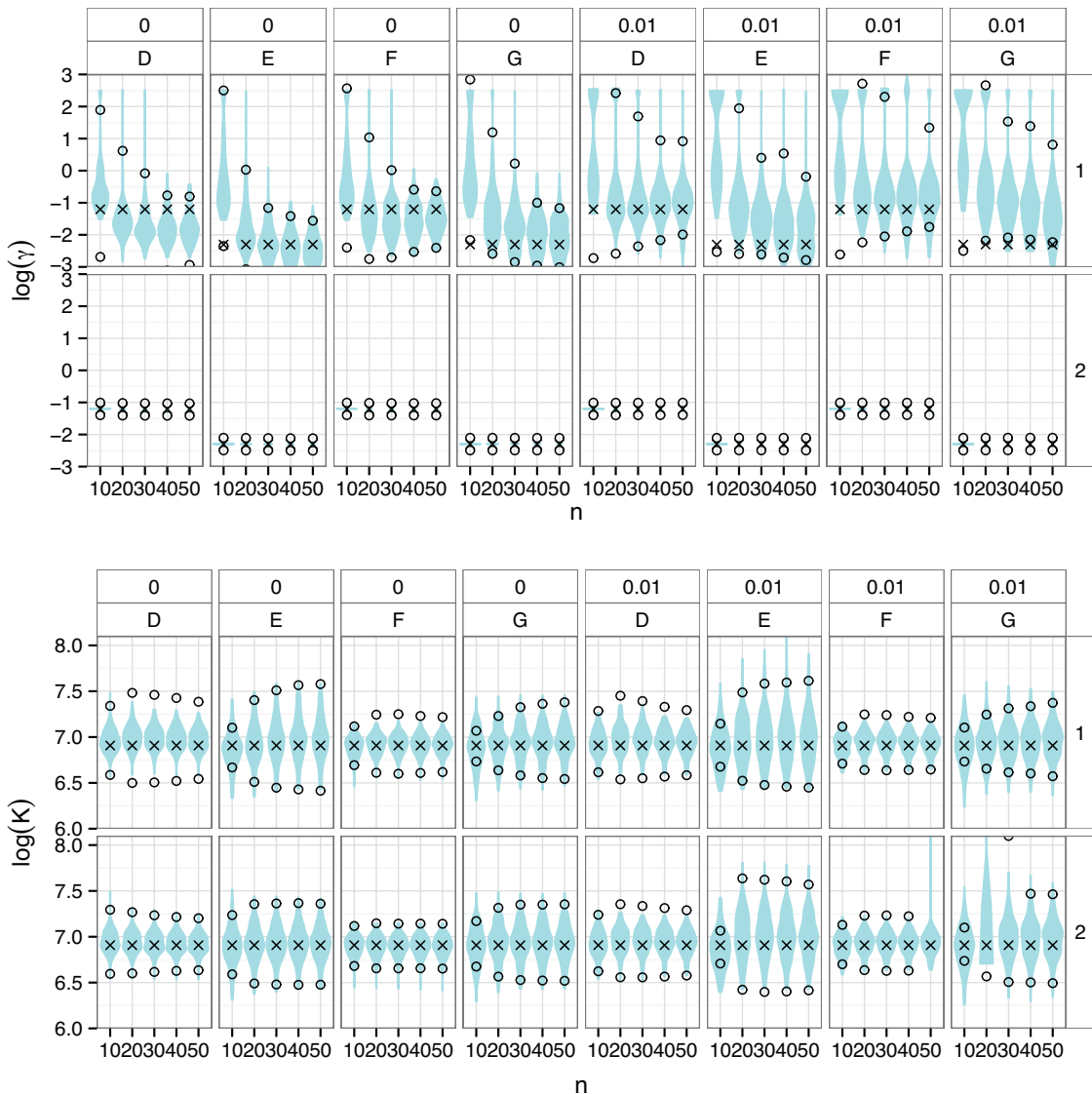


**Fig. E.10.** Violin plots of  $\log \gamma$  (top) and  $\log K$  (bottom), for step-wise change in  $K$ , for different sample sizes, sampling error and prior distribution on  $\beta$ . The violins are log values of the mean posterior distribution from 200 time series for each combination of sample size  $n$ , sampling variance  $\tau^2$  and prior  $\pi(\beta)$ . The points are the mean upper and lower 95% credible intervals of the posterior distributions ( $\circ$ ). The crosses are the true values ( $\times$ ). The parameter values are  $r_1 = 0.2$ ,  $K = 1000$  and  $\sigma_e^2 = 0.01$ . The change in carrying capacity occurs at  $s = 6$  for all values of  $n$ . The columns with '0' and '0.01' indicate the value of  $\tau^2$ , D–G are the cases described in the text and illustrated in Fig. 2, while in row 1  $\log \beta \sim N(0, 20)$  and row 2  $\log \beta \sim N(\log \gamma, 0.01)$ .

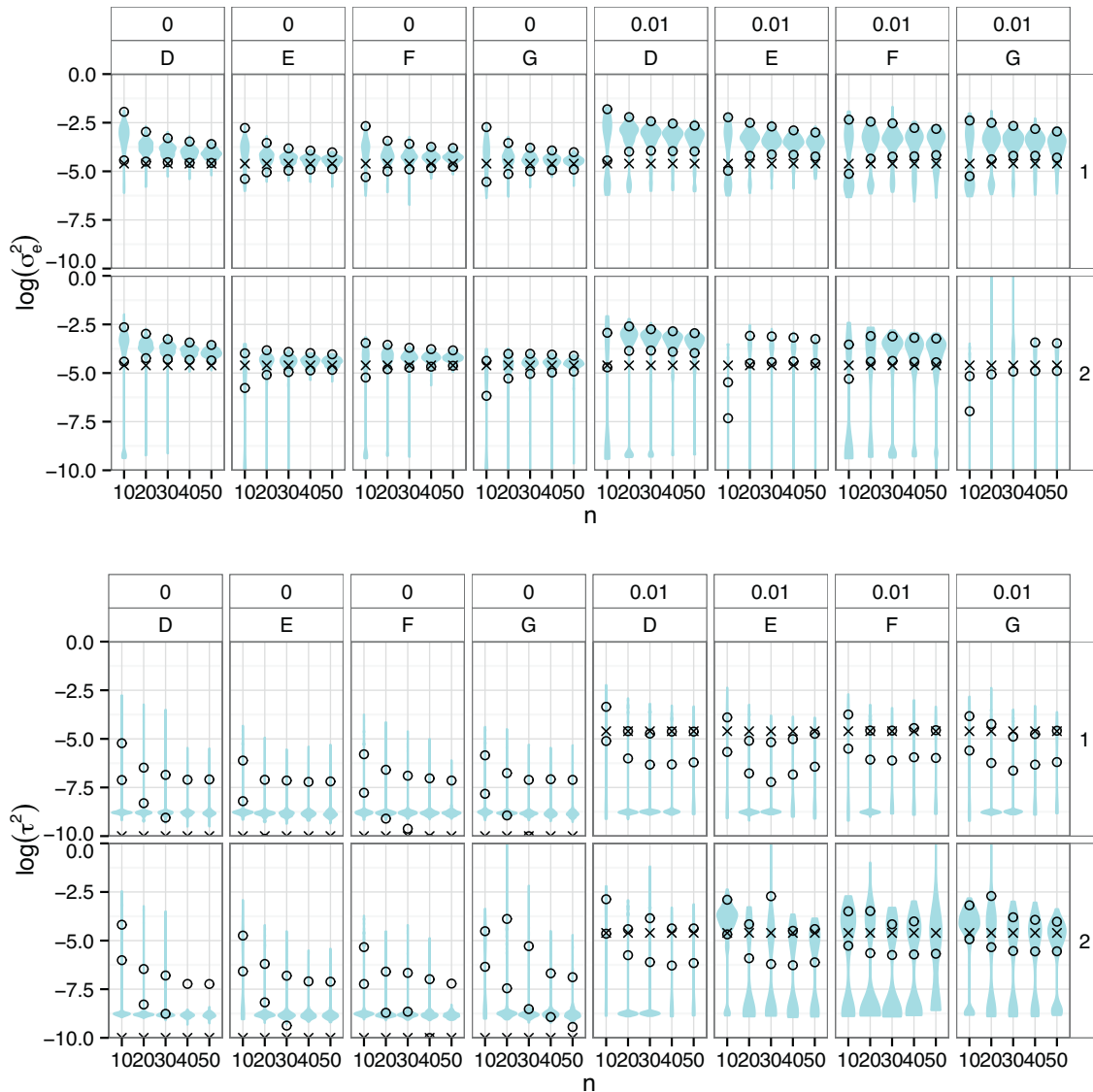


**Fig. E.11.** Violin plots of  $\log \sigma_e^2$  (top) and  $\log \tau^2$  (bottom), for step-wise change in  $K$ , for different sample sizes, sampling error and prior distribution on  $\beta$ . The violins are log values of the mean posterior distribution from 200 time series for each combination of sample size  $n$ , sampling variance  $\tau^2$  and prior  $\pi(\beta)$ . The points are the mean upper and lower 95% credible intervals of the posterior distributions ( $\circ$ ). The crosses are the true values ( $\times$ ). The parameter values are  $r_1 = 0.2$ ,  $K = 1000$  and  $\sigma_e^2 = 0.01$ . The change in carrying capacity occurs at  $s = 6$  for all values of  $n$ . The columns with '0' and '0.01' indicate the value of  $\tau^2$ , D–G are the cases described in the text and illustrated in Fig. 2, while in row 1  $\log \beta \sim N(0, 20)$  and row 2  $\log \beta \sim N(\log \gamma, 0.01)$ .

## Appendix F. Additional results for gradual changes in carrying capacity

**Table F.8**

Posterior means and credible intervals from the analysis of the four sample cases of gradual changes in  $K$ , illustrated in Fig. 3. In H and I,  $\kappa = 0.98$ . In J and K,  $\kappa = 1.02$ . In H and J,  $\theta = 1.5$ . In I and K,  $\theta = 0.5$ . The numbering of the cases indicates the prior distribution on  $\log \beta$  used: (1)  $N(0, 5)$  (2)  $N(\ln \gamma, 0.01)$ . The other parameter values are  $r_1 = 0.2$ ,  $K = 1000$ ,  $\sigma_e^2 = 0.01$  and  $\tau^2 = 0.0$ .

Case	$\gamma$	$K$		$\kappa$		$\sigma_e^2$		$\tau^2$		
		Mean	Cred.int	Mean	Cred.int	Mean	Cred.int	Mean	Cred.int	
H1	0.286	0.104, 0.547	1110.0	905.4, 1344.9	0.976	0.970, 0.982	0.011	0.007, 0.017	0.000	0.000, 0.001
H2	0.302	0.248, 0.364	1104.2	931.3, 1296.0	0.976	0.970, 0.981	0.011	0.007, 0.016	0.000	0.000, 0.001
I1	0.067	0.014, 0.162	1317.0	790.0, 2020.7	0.977	0.965, 0.988	0.007	0.004, 0.010	0.000	0.000, 0.001
I2	0.099	0.081, 0.120	1275.4	925.6, 1727.8	0.977	0.968, 0.987	0.007	0.004, 0.010	0.000	0.000, 0.001
J1	0.774	0.337, 1.430	940.3	864.4, 1023.2	1.022	1.019, 1.025	0.013	0.007, 0.022	0.000	0.000, 0.001
J2	0.311	0.255, 0.377	952.5	820.0, 1116.6	1.022	1.016, 1.027	0.010	0.006, 0.014	0.000	0.000, 0.001
K1	0.382	0.150, 0.718	988.5	830.8, 1134.4	1.010	1.005, 1.016	0.012	0.007, 0.020	0.000	0.000, 0.001
K2	0.102	0.083, 0.124	1041.9	714.8, 1457.6	1.011	0.999, 1.023	0.010	0.007, 0.015	0.000	0.000, 0.001

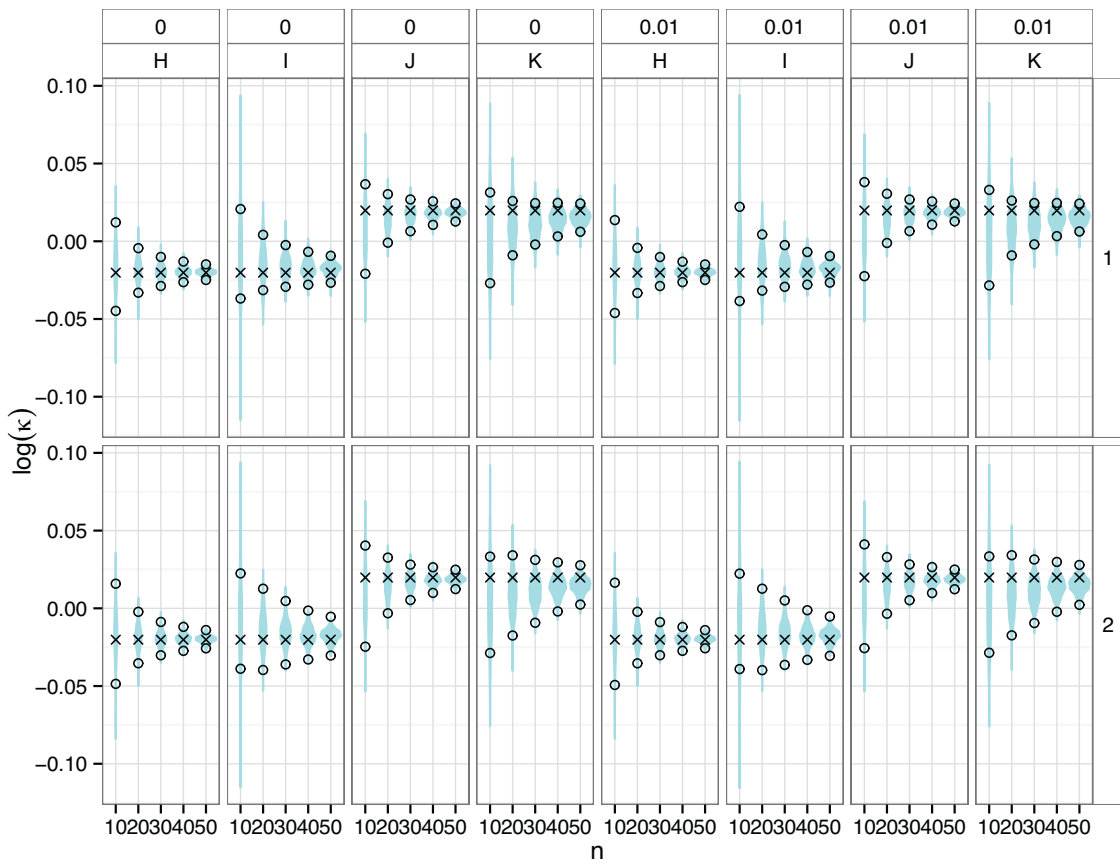


**Fig. F.12.** Violin plots of  $\log \kappa$  for gradual change in  $K$ , for different sample sizes, sampling error and prior distribution on  $\beta$ . The violins are  $\log$  values of the mean posterior distribution from 500 time series for each combination of sample size  $n$ , sampling variance  $\tau^2$  and prior  $\pi(\beta)$ . The points are the mean upper and lower 95% credible intervals of the posterior distributions ( $\circ$ ). The crosses are the true values ( $\times$ ). The parameter values are  $r_1 = 0.2$ ,  $K = 1000$  and  $\sigma_\gamma^2 = 0.01$ . The change in carrying capacity is 2% annually, either decreasing (H and I) or increasing (J and K). The columns with '0' and '0.01' indicate the value of  $\tau^2$ , H–K are the cases described in the text and illustrated in Fig. 3, while in row 1  $\log \beta \sim N(0, 20)$  and row 2  $\log \beta \sim N(\log \gamma, 0.01)$ .

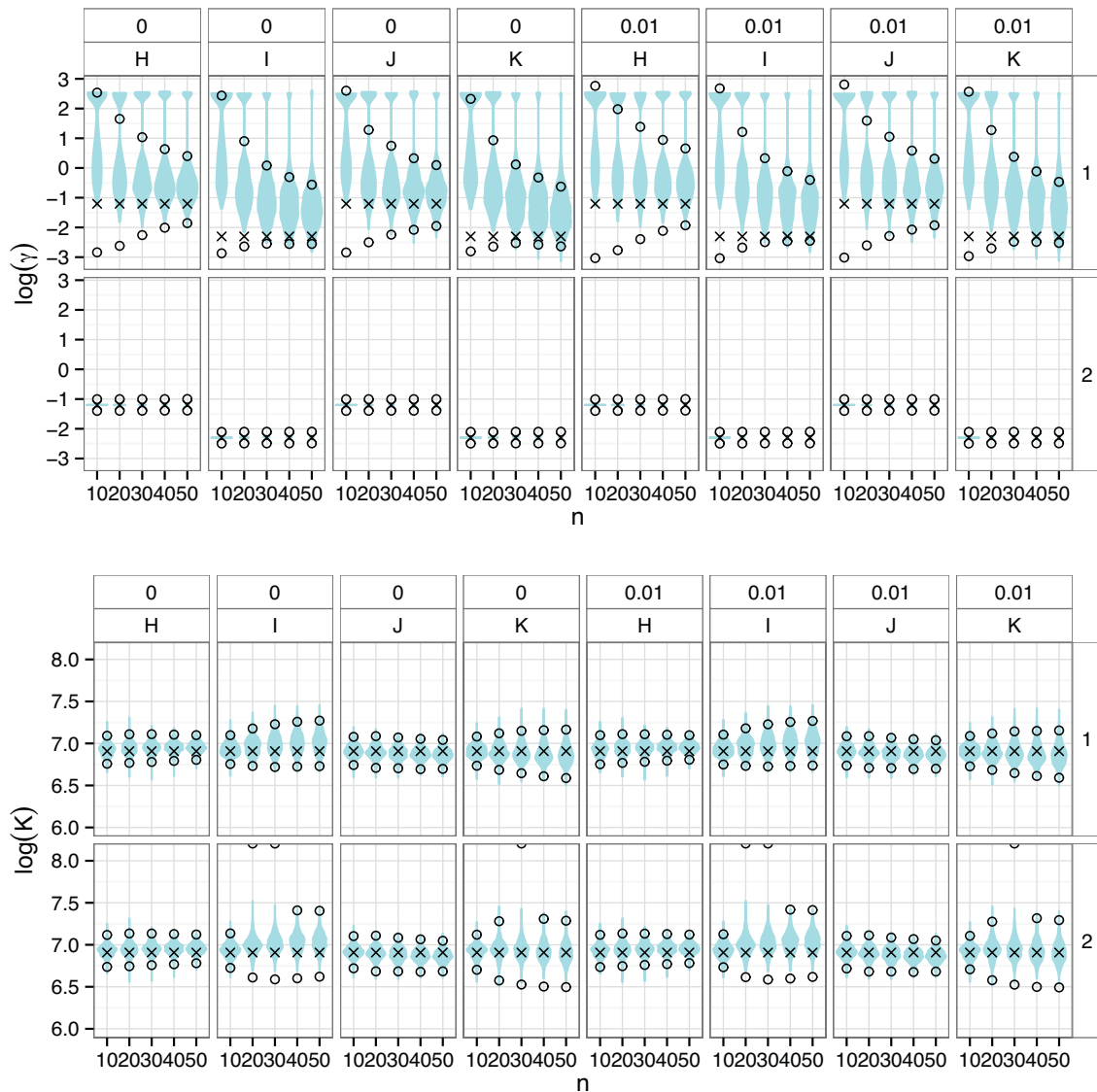


**Fig. F.13.** Violin plots of  $\log \gamma$  (top) and  $\log K$  (bottom), for gradual change in  $K$ , for different sample sizes, sampling error and prior distribution on  $\beta$ . The violins are log values of the mean posterior distribution from 500 time series for each combination of sample size  $n$ , sampling variance  $\tau^2$  and prior  $\pi(\beta)$ . The points are the mean upper and lower 95% credible intervals of the posterior distributions ( $\circ$ ). The crosses are the true values ( $\times$ ). The parameter values are  $r_1 = 0.2$ ,  $K = 1000$  and  $\sigma_\beta^2 = 0.01$ . The change in carrying capacity is 2% annually, either decreasing (H and I) or increasing (J and K). The columns with '0' and '0.01' indicate the value of  $\tau^2$ , H–K are the cases described in the text and illustrated in Fig. 3, while in row 1  $\log \beta \sim N(0, 20)$  and row 2  $\log \beta \sim N(\log \gamma, 0.01)$ .

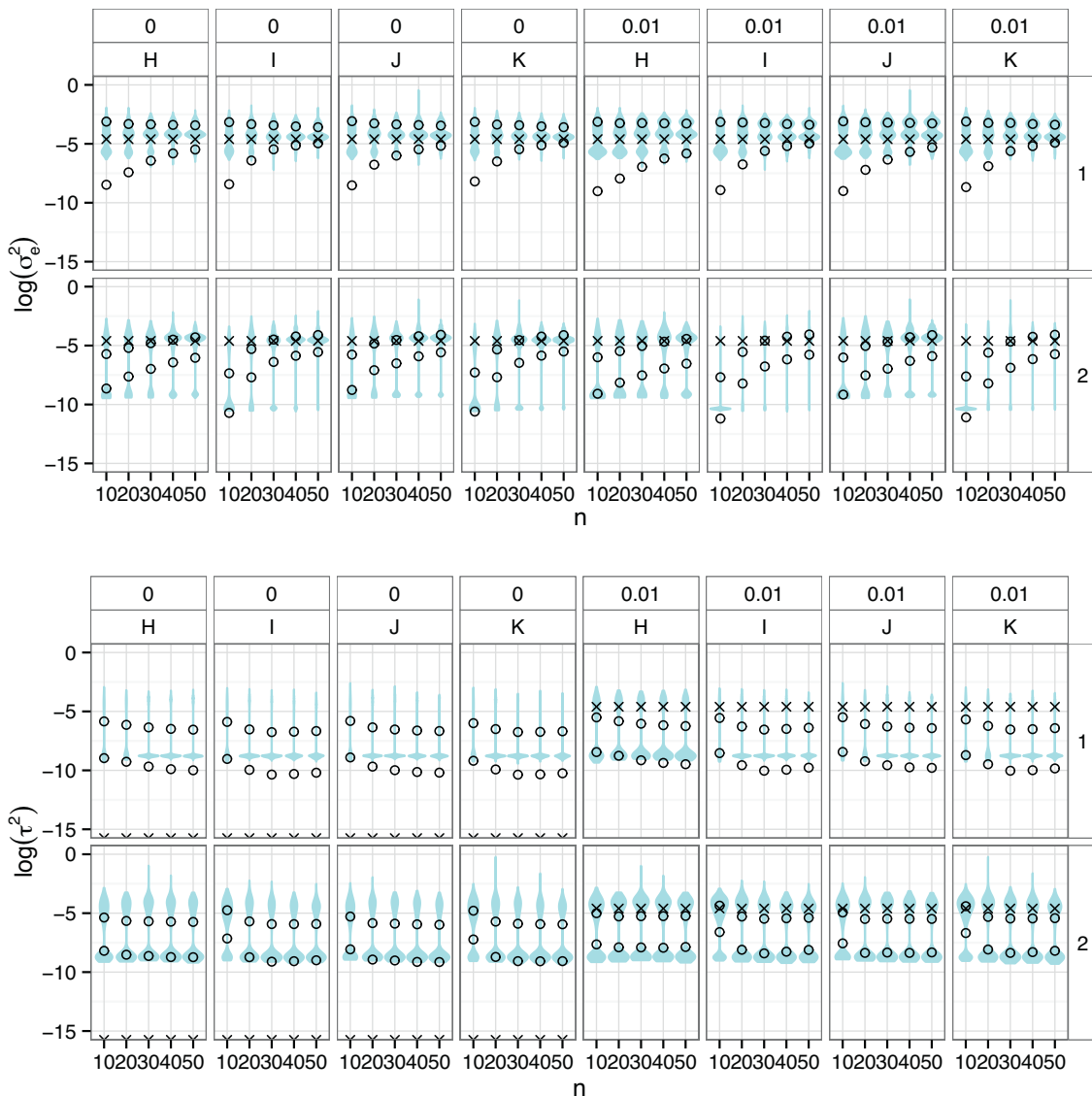


**Fig. F.14.** Violin plots of  $\log \sigma_e^2$  (top) and  $\log \tau^2$  (bottom), for gradual change in  $K$ , for different sample sizes, sampling error and prior distribution on  $\beta$ . The violins are log values of the mean posterior distribution from 500 time series for each combination of sample size  $n$ , sampling variance  $\tau^2$  and prior  $\pi(\beta)$ . The points are the mean upper and lower 95% credible intervals of the posterior distributions ( $\circ$ ). The crosses are the true values ( $\times$ ). The parameter values are  $r_1 = 0.2$ ,  $K = 1000$  and  $\sigma_e^2 = 0.01$ . The change in carrying capacity is 2% annually, either decreasing (H and I) or increasing (J and K). The columns with '0' and '0.01' indicate the value of  $\tau^2$ , H-K are the cases described in the text and illustrated in Fig. 3, while in row 1  $\log \beta \sim N(0, 20)$  and row 2  $\log \beta \sim N(\log \gamma, 0.01)$ .

## Appendix G. Sample code for estimating step-wise change in carrying capacity using INLA

```

# Need to have the INLA package installed, see www.r-inla.org
require(INLA)

# The observed population counts, time points and time point
# of change in carrying capacity

y <- "YOUR OBSERVATIONS"
time <- "THE TIME POINTS OF OBSERVATIONS"
s <- "THE TIME POINT OF step-wise CHANGE IN CARRYING CAPACITY"

# Restructure 'time' to start at zero and begin at zero again at time 's'
time_std <- c(time[1:(which(time==s)-1)]-time[1],time[which(time==s):length(time)]-s)

# 'group' is used to whether the observation is before or after the change
group <- rep(c(1,2),c(which(time_std==0)[2]-1,length(time_std)-which(time_std==0)[2]+1))

# Indicator function, which is multiplied with alpha_1
step <- as.factor(group-1)

# The following is the default wage prior on log(beta). NOTE: INLA denote
# this parameter as 'phi', see www.r-inla.org

hyper=list(
  phi=list(
    prior="normal",
    param=c(0, 0.2), # c('mean','precision')
    initial=-1,
    fixed=FALSE
  )
)
formula = y ~ 1 + step + f(time_std, model="ou", replicate=group, hyper=hyper)
result = inla(formula, data = data.frame(y, time_std, step), control.compute=list(dic=TRUE))
summary(result)

# Posterior means of the diffusion parameters
alpha_0_hat <- result$summary.fixed[1,1]
alpha_1_hat <- result$summary.fixed[2,1]
beta_hat <- result$summary.hyperpar[3,1]
varepsilon_hat <- result$summary.hyperpar[2,1]
varsigma_hat <- result$summary.hyperpar[1,1]
X_hat <- result$summary.fitted.values[,1]

# If demographic variance is available, set it to the estimated value
sd2_hat <- 0

# The corresponding biological parameters, using point estimates
tau2_hat <- 1/varsigma_hat
se2_hat <- 2*beta_hat/varepsilon_hat-
  sd2_hat*sum(exp(-X_hat[-length(X_hat)])*(1-exp(-2*beta_hat*diff(time))))/sum((1-exp(-2*beta_hat*diff(time))))
kappa_hat <- exp(alpha_1_hat)
require(gsl)
K_hat <- exp(lambert_W0(diff(range(time))*sd2_hat*exp(-alpha_0_hat-1/varepsilon_hat)/
  (2*beta_hat*(s+(range(time)[2]-s)*kappa_hat)))+alpha_0_hat+1/varepsilon_hat[,2])
K_bar <- K_hat*(s+(range(time)[2]-s)*kappa_hat)/range(time)[2]
gamma_hat <- beta_hat-sd2_hat/(2*K_bar)
cbind(gamma_hat,K_hat,kappa_hat,se2_hat,sd2_hat,tau2_hat)

# Function that computes the point estimates (mean and mode) of the biological
# parameters, in addition to upper and lower 95% credible intervals sampling

```

```

# from the posterior distributions of the diffusion parameters
aux_inla <- function(result, sd2=0, time, s)
{
  sd2_hat=sd2

  tmp.results <- matrix(nrow = 1, ncol = 21)
  colnames(tmp.results) = c(rep(c("mean", "mode", "2.5% cred.int", "97.5% cred.int"),5),"DIC")
  tmp.alpha0 <- inla.rmarginal(n = 1000, marginal = result$marginals.fixed$(Intercept)')
  tmp.alpha1 <- inla.rmarginal(n = 1000, marginal = result$marginals.fixed$step)
  tmp.hyper <- inla.hyperpar.sample(n = 1000, result = result)

  X_hat <- result$summary.fitted.values[,1]
  beta_hat <- result$summary.hyperpar[3,1]
  tmp.se2 <- 2*tmp.hyper[,3]/tmp.hyper[,2]-
    sd2_hat*sum(exp(-X_hat[-length(X_hat)])*(1-exp(-2*beta_hat*diff(time))))/sum((1-exp(-2*beta_hat*diff(time))))
  tmp.results[1, 13] <- mean(tmp.se2)
  tmp.se2.dens <- density(tmp.se2)
  tmp.results[1, 14] <- tmp.se2.dens$x[which.max(tmp.se2.dens$y)]
  tmp.results[1, 15:16] <- quantile(tmp.se2, probs=c(0.025, 0.975))
  tmp.tau2 <- 1/tmp.hyper[,1]
  tmp.results[1, 17] <- mean(tmp.tau2)
  tmp.tau2.dens <- density(tmp.tau2)
  tmp.results[1, 18] <- tmp.tau2.dens$x[which.max(tmp.tau2.dens$y)]
  tmp.results[1, 19:20] <- quantile(tmp.tau2, probs=c(0.025, 0.975))
  tmp.kappa <- exp(tmp.alpha1)
  tmp.results[1, 9] <- mean(tmp.kappa)
  tmp.kappa.dens <- density(tmp.kappa)
  tmp.results[1, 10] <- tmp.kappa.dens$x[which.max(tmp.kappa.dens$y)]
  tmp.results[1, 11:12] <- quantile(tmp.kappa, probs=c(0.025, 0.975))
  tmp.K <- exp(lambert_W0(diff(range(time))*sd2_hat*exp(-tmp.alpha0-1/tmp.hyper[,2])/
    (2*tmp.hyper[,3]*(s+(range(time)[2]-s)*tmp.kappa)))+tmp.alpha0+1/tmp.hyper[,2])
  tmp.results[1, 5] <- mean(tmp.K)
  tmp.K.dens <- density(tmp.K)
  tmp.results[1, 6] <- tmp.K.dens$x[which.max(tmp.K.dens$y)]
  tmp.results[1, 7:8] <- quantile(tmp.K, probs=c(0.025, 0.975))
  K_bar <- mean(tmp.K)*(s+(range(time)[2]-s)*mean(tmp.kappa))/range(time)[2]
  tmp.gamma <- tmp.hyper[,3]-sd2_hat/(2*K_bar)
  tmp.results[1, 1] <- mean(tmp.gamma)
  tmp.gamma.dens <- density(tmp.gamma)
  tmp.results[1, 2] <- tmp.gamma.dens$x[which.max(tmp.gamma.dens$y)]
  tmp.results[1, 3:4] <- quantile(tmp.gamma, probs=c(0.025, 0.975))
  tmp.results[1, 21] <- result$dic$dic
  return(tmp.results)
}

aux_inla(result, sd2, time, s) #output is gamma, K, kappa, se2, tau2 and DIC

```

## Appendix H. Sample code for estimating gradual change in carrying capacity using INLA

```

# Need to have the INLA package installed, see www.r-inla.org
require(INLA)

# The observed population counts, time points and time point
# of change in carrying capacity

y <- "YOUR OBSERVATIONS"
time <- "THE TIME POINTS OF OBSERVATIONS"

# Restructure 'time' to start at zero
time_std <- c(time-time[1])

# Trend
trend <- time_std

# The following is the default wage prior on log(beta). NOTE: INLA denote
# this parameter as 'phi', see www.r-inla.org

hyper=list(
  phi=list(
    prior="normal",
    param=c(0, 0.2), # c('mean','precision')
    initial=-1,
    fixed=FALSE
  )
)

formula = y ~ 1 + trend + f(time_std, model="ou", hyper=hyper)
result = inla(formula, data = data.frame(y, time_std, trend), control.compute=list(dic=TRUE))
summary(result)

# Posterior means of the diffusion parameters
alpha_0_hat <- result$summary.fixed[1,1]
alpha_1_hat <- result$summary.fixed[2,1]
beta_hat <- result$summary.hyperpar[3,1]
varepsilon_hat <- result$summary.hyperpar[2,1]
varsigma_hat <- result$summary.hyperpar[1,1]
X_hat <- result$summary.fitted.values[,1]

# If demographic variance is available, set it to the estimated value
sd2_hat <- 0

# The corresponding biological parameters, using point estimates
tau2_hat <- 1/varsigma_hat
se2_hat <- 2*beta_hat/varepsilon_hat-
  sd2_hat*sum(exp(-X_hat[-length(X_hat)])*(1-exp(-2*beta_hat*diff(time))))/sum((1-exp(-2*beta_hat*diff(time))))
kappa_hat <- exp(alpha_1_hat)

require(gsl)

K_hat <- exp(lambert_W0(diff(range(time))*sd2_hat*exp(-alpha_0_hat-1/varepsilon_hat)/
  (2*beta_hat*sum(kappa_hat*time_std[-length(time_std)])))+alpha_0_hat+1/varepsilon_hat)

K_bar <- K_hat*sum(kappa_hat*time_std[-length(time_std)])/range(time)[2]
gamma_hat <- beta_hat-sd2_hat/(2*K_bar)
cbind(gamma_hat,K_hat,kappa_hat,se2_hat,sd2_hat,tau2_hat)

# Function that computes the point estimates (mean and mode) of the biological
# parameters, in addition to upper and lower 95% credible intervals sampling
# from the posterior distributions of the diffusion parameters
aux_inla <- function(result, sd2=0, time)
{

```

```

sd2_hat=sd2

tmp.results <- matrix(nrow = 1, ncol = 21)

colnames(tmp.results) = c(rep(c("mean", "mode", "2.5% cred.int", "97.5% cred.int"),5),"DIC")
tmp.alpha0 <- inla.rmarginal(n = 1000, marginal = result$marginals.fixed$(Intercept)')
tmp.alpha1 <- inla.rmarginal(n = 1000, marginal = result$marginals.fixed$trend)
tmp.hyper <- inla.hyperpar.sample(n = 1000, result = result)
X_hat <- result$summary.fitted.values[,1]
beta_hat <- result$summary.hyperpar[3,1]
tmp.se2 <- 2*tmp.hyper[,3]/tmp.hyper[,2]-
  sd2_hat*sum(exp(-X_hat)[-length(X_hat)]*(1-exp(-2*beta_hat*diff(time))))/sum((1-exp(-2*beta_hat*diff(time))))
tmp.results[1, 13] <- mean(tmp.se2)
tmp.se2.dens <- density(tmp.se2)
tmp.results[1, 14] <- tmp.se2.dens$x[which.max(tmp.se2.dens$y)]
tmp.results[1, 15:16] <- quantile(tmp.se2, probs=c(0.025, 0.975))
tmp.tau2 <- 1/tmp.hyper[,1]
tmp.results[1, 17] <- mean(tmp.tau2)
tmp.tau2.dens <- density(tmp.tau2)
tmp.results[1, 18] <- tmp.tau2.dens$x[which.max(tmp.tau2.dens$y)]
tmp.results[1, 19:20] <- quantile(tmp.tau2, probs=c(0.025, 0.975))
tmp.kappa <- exp(tmp.alpha1)
tmp.results[1, 9] <- mean(tmp.kappa)
tmp.kappa.dens <- density(tmp.kappa)
tmp.results[1, 10] <- tmp.kappa.dens$x[which.max(tmp.kappa.dens$y)]
tmp.results[1, 11:12] <- quantile(tmp.kappa, probs=c(0.025, 0.975))
tmp.K <- exp(lambert_W0(diff(range(time))*sd2_hat*exp(-tmp.alpha0-1/tmp.hyper[,2])/
  (2*tmp.hyper[,3]*sum(mean(tmp.kappa)^time[-length(time)])))+tmp.alpha0+1/tmp.hyper[,2])
tmp.results[1, 5] <- mean(tmp.K)
tmp.K.dens <- density(tmp.K)
tmp.results[1, 6] <- tmp.K.dens$x[which.max(tmp.K.dens$y)]
tmp.results[1, 7:8] <- quantile(tmp.K, probs=c(0.025, 0.975))
K_bar <- mean(tmp.K)*sum(mean(tmp.kappa)^time[-length(time)])/range(time)[2]
tmp.gamma <- tmp.hyper[,3]-sd2_hat/(2*K_bar)
tmp.results[1, 1] <- mean(tmp.gamma)
tmp.gamma.dens <- density(tmp.gamma)
tmp.results[1, 2] <- tmp.gamma.dens$x[which.max(tmp.gamma.dens$y)]
tmp.results[1, 3:4] <- quantile(tmp.gamma, probs=c(0.025, 0.975))
tmp.results[1, 21] <- result$dic$dic
return(tmp.results)
}

aux_inla(result, sd2, time) #output is gamma, K, kappa, se2, tau2 and DIC

```

## Appendix I. Comparison of results from Dennis and Ponciano (2014) with INLA

**Table I.9** Comparison of results from Dennis and Ponciano (2014) using restricted maximum likelihood (REML) with estimates using INLA.

Case	n	Method	$\beta(\theta)$	$\alpha(\mu)$			$\sigma_e^2(\beta)$			$\tau^2$		
				Mean	Mode	Conf/Cred.int	Mean	Mode	Conf/Cred.int	Mean	Mode	Conf/Cred.int
Bobcats, Idaho	22	REML	1.26	(3.913 $\times 10^{-7}$ , 20.2)	6.79	(6.61, 6.97)	0.272	(7.43 $\times 10^{-3}$ , 3.94)	7.48 $\times 10^{-4}$	(9.14 $\times 10^{-10}$ , 8.47 $\times 10^{-2}$ )	1.01 $\times 10^{-1}$	(5.61 $\times 10^{-2}$ , 1.70 $\times 10^{-1}$ )
		INLA	9.27	7.5 $\times 10^{-3}$	(1.340 $\times 10^{-2}$ , 74.7)	6.80	(6.66, 6.93)	3.039 $\times 10^{-3}$	0	(1.682 $\times 10^{-6}$ , 0.0196)		
Bobcats, Maine	40	REML	0.877	(0.0226, 10.3)	5.78	(5.47, 6.08)	0.735	(0.02, 0.240)	4.75 $\times 10^{-3}$	(1.79 $\times 10^{-8}$ , 3.34 $\times 10^{-1}$ )	1.42 $\times 10^{-4}$	(1.422 $\times 10^{-5}$ , 6.90 $\times 10^{-4}$ )
		INLA	1.448	0.887	(0.530, 5.21)	5.78	(5.48, 6.09)	1.162	0.854	(0.466, 2.55)		
Elk, Wyoming	22	REML	0.868	(0.229, 19.3)	7.29	(7.14, 7.44)	0.0990	(0.0296, 1.45)	9.80 $\times 10^{-9}$	(2.93 $\times 10^{-11}$ , 1.222 $\times 10^{-3}$ )	4.01 $\times 10^{-5}$	(1.51 $\times 10^{-5}$ , 9.722 $\times 10^{-4}$ )
		INLA	1.773	0.740	(0.413, 9.01)	7.29	(7.14, 7.45)	0.145	0.0877	(0.0453, 0.398)		
Grasshoppers, Montana	39	REML	0.722	(0.272, 2.01)	1.56	(1.31, 1.82)	0.347	(0.160, 0.752)	2.27 $\times 10^{-7}$	(3.81 $\times 10^{-8}$ , 2.27 $\times 10^{-5}$ )	1.61 $\times 10^{-4}$	4.36 $\times 10^{-5}$
		INLA	0.873	0.670	(0.418, 1.86)	1.56	(1.31, 1.82)	0.415	0.334	(0.188, 0.856)		

## Appendix J. R-code used to produce this article

**Grey Heron example:** <http://www.math.ntnu.no/~erikblys/R-code/A2/grey-heron/>

**Step-wise change in growth rate:** <http://www.math.ntnu.no/~erikblys/R-code/A2/growth-rate/>

**Step-wise change in carrying capacity:** <http://www.math.ntnu.no/~erikblys/R-code/A2/carrying-capacity-step/>

**Gradual change in carrying capacity:** <http://www.math.ntnu.no/~erikblys/R-code/A2/carrying-capacity-gradual/>

**Examples from section S6:** <http://www.math.ntnu.no/~erikblys/R-code/A2/appendix-s6/>

## References

- Bjørnstad, O.N., Grenfell, B.T., 2001. Noisy clockwork: time series analysis of population fluctuations in animals. *Science* 293 (5530), 638–643.
- Bolker, B.M., Gardner, B., Maunder, M., Berg, C.W., Brooks, M., Comita, L., Crone, E., Cubaynes, S., Davies, T., de Valpine, P., Ford, J., Gimenez, O., Kry, M., Kim, E.J., Lennert-Cody, C., Magnusson, A., Martell, S., Nash, J., Nielsen, A., Regetz, J., Skaug, H., Zipkin, E., 2013. Strategies for fitting nonlinear ecological models in r, ad model builder, and bugs. *Methods Ecol. Evolut.* 4 (6), 501–512, <http://dx.doi.org/10.1111/2041-210X.12044>
- Brook, B.W., Traill, L.W., Bradshaw, C.J.A., 2006. Minimum viable population sizes and global extinction risk are unrelated. *Ecol. Lett.* 9 (4), 375–382.
- Dennis, B., Ponciano, J.M., 2006. Density dependent state-space model for population abundance data with unequal time intervals. *Ecology* 95 (8), 2069–2076.
- Dennis, B., Ponciano, J.M., Lele, S.R., Taper, M.L., Staples, D.F., 2006. Estimating density dependence, process noise, and observation error. *Ecol. Monogr.* 76 (3), 323–341.
- Engen, S., Bakke, Ø., Islam, A., 1998. Demographic and environmental stochasticity – concepts and definitions. *Biometrics* 54 (3), 840–846.
- Gilpin, M.E., Ayala, F.J., 1973. Global models of growth and competition. *Proc. Natl. Acad. Sci. U. S. A.* 70 (12), 3590–3593.
- Gompertz, B., 1825. On the nature of the function expressive of the law of human mortality, and on a new mode of determining the value of life contingencies. *Philos. Trans. R. Soc. Lond.* 115, 513–583.
- Herrando-Pérez, S., Delean, S., Brook, B.W., Bradshaw, C.J., 2012. Density dependence: an ecological tower of babel. *Oecologia* 170 (3), 585–603.
- Hintze, J.L., Nelson, R.D., 1998. Violin plots: a box plot-density trace synergism. *Am. Stat.* 52 (2), 181–184.
- Humbert, J.-Y., Scott Mills, L., Horne, J.S., Dennis, B., 2009. A better way to estimate population trends. *Oikos* 118 (12), 1940–1946.
- Ives, A.R., Abbott, K.C., Ziebarth, N.L., 2010. Analysis of ecological time series with ARMA(p, q) models. *Ecology* 91 (3), 858–871.
- Karlin, S., Taylor, H.M., 1981. A Second Course in Stochastic Processes. Academic Press, New York.
- Lande, R., Engen, S., Sæther, B.-E., 2002. Estimating density dependence in time-series of age-structured populations. *Philos. Trans. R. Soc. B: Biol. Sci.* 357 (1425), 1179–1184.
- Lande, R., Engen, S., Sæther, B.-E., 2003. Stochastic Population Dynamics in Ecology and Conservation. Oxford University Press, Oxford.
- Lebreton, J.-D., Gimenez, O., 2013. Detecting and estimating density dependence in wildlife populations. *J. Wildl. Manag.* 77 (1), 12–23.
- Margalida, A., Colomer, M.À., Oro, D., 2014. Man-induced activities modify demographic parameters in a long-lived species: effects of poisoning and health policies. *Ecol. Appl.* 24 (3), 436–444.
- May, R.M., 1981. Models for single populations. *Theor. Ecol. Princ. Appl.* 2, 5–17.
- NERC Centre for Population Biology, Imperial College, 2010. The Global Population Dynamics Database Version 2. <http://www.sw.ic.ac.uk/cpb/cpb/gpdd.html>
- Pedersen, M.W., Berg, C.W., Thygesen, U.H., Nielsen, A., Madsen, H., 2011. Estimation methods for nonlinear state-space models in ecology. *Ecol. Model.* 222 (8), 1394–1400.
- Plummer, M., 2003. JAGS: a program for analysis of Bayesian graphical models using Gibbs sampling. In: Proceedings of the 3rd International Workshop on..., <http://www.ci.tuwien.ac.at/Conferences/DSC-2003/Drafts/Plummer.pdf>, ISSN 1609–395X.
- R Core Team, 2014. R: A Language and Environment for Statistical Computing. <http://www.r-project.org/>
- Rue, H., Martino, S., Chopin, N., 2009. Approximate Bayesian inference for latent Gaussian models by using integrated nested Laplace approximations. *J. R. Stat. Soc. Ser. B* 71 (2), 319–392.
- Sæther, B.-E., Engen, S., Lande, R., Arcese, P., Smith, J., 2000. Estimating the time to extinction in an island population of song sparrows. *Proc. R. Soc. B: Biol. Sci.* 267 (1443), 621.

- Seber, G.A.F., 1982. *The Estimation of Animal Abundance*. Griffin, London.
- Solbu, E.B., Engen, S., Diserud, O.H., 2013. Changing environments causing time delays in population dynamics. *Math. Biosci.* 244 (2), 213–223.
- Staudenmayer, J., Buonaccorsi, J.P., 2005. Measurement error in linear autoregressive models. *J. Am. Stat. Assoc.* 100 (471), 841–852.
- Turchin, P., 2003. *Complex Population Dynamics: A Theoretical/Empirical Synthesis, vol. 35*. Princeton University Press.
- Wang, G., 2007. On the latent state estimation of nonlinear population dynamics using Bayesian and non-Bayesian state-space models. *Ecol. Model.* 200 (3), 521–528.